IN-16-CR
57112
P 70

NASA CONTRACTOR REPORT

PERFORMANCE ANALYSIS OF ADVANCED SPACECRAFT TPS

Willliam C. Pitts

Eloret Institute
3788 Fabian Way
Palo Alto, CA 94303

Prepared for

Ames Research Center
under **Cooperative Agreement NCC2-434**

National Aeronautics and
Space Administration

Ames Research Center
Moffett Field, California 94035

NASA CONTRACTOR REPORT

PERFORMANCE ANALYSIS OF ADVANCED SPACECRAFT TPS

William C. Pitts

CONTRACT NAS2– 434

NASA

1. Report No.	2. Government Accession No.	3. Recipient's Catalog No.
4. Title and Subtitle Performance Analysis of Advanced Spacecraft TPS		5. Report Date 17 December 1991 6. Performing Organization Code
7. Author(s) William C. Pitts		8. Performing Organization Report No. 10. Work Unit No.
9. Performing Organization Name and Address Eloret Institute 3788 Fabian Way Palo Alto, CA 94303		11. Contract or Grant No. NCC2-434
12. Sponsoring Agency Name and Address National Aeronautics and Space Administration, Washington, D.C. 20456		13. Type of Report and Period Covered 8/1/86 - 9/30/91 14. Sponsoring Agency Code

15. Supplementary Notes
Point of Contact: Dr. Daniel J. Rasky
c/o 234-1 NASA Ames Research Center, Moffett Field, CA 94035.

16. Abstract

Spacecraft entering a planetary atmosphere require a very sophisticated thermal protection system. The materials used must be tailored to each specific vehicle based on its planned mission profiles. Starting with the Space Shuttle, many types of ceramic insulation with various combinations of thermal properties have been developed by others. The development of two new materials is described: A Composite Flexible Blanket Insulation which has a significantly lower effective thermal conductivity than other ceramic blankets; and a Silicon Matrix Composite which has application at high temperature locations such as wing leading edges. Also, a systematic study is described that considers the application of these materials for a proposed Personnel Launch System which shows how most of these available ceramic materials would perform during atmospheric entry of this vehicle. The options and choice of material are discussed. Other specific applications and performance of these thermal protection materials are discussed.

17. Key Words (Suggested by Author(s))	18. Distribution Statement
Thermal Protection Space Shuttle Ceramic Insulation Composites	Unclassified, Unlimited

19. Security Classif. (of this report)	20. Security Classif. (of this page)	21. No. of Pages	22. Price*
Unclassified	Unclassified	70	

*For sale by the National Technical Information Service, Springfield, Virginia 22161

PERFORMANCE ANALYSIS OF ADVANCED SPACECRAFT TPS

Final Technical Report

for the period
August 1, 1986 - September 30, 1991

Cooperative Agreement NCC2-434

Submitted to

National Aeronautics and Space Administration
Ames Research Center
Moffett Field, California 94035

Thermal Protection Materials Branch
Dr. Daniel J. Rasky, Chief and Technical Monitor

Thermosciences Division
Dr. Jim Arnold, Chief

Prepared by

ELORET INSTITUTE
1178 Maraschino Drive
Sunnyvale, CA 94087
Phone: 408 730-8422 and 415 493-4710
Telefax: 408-730-1441
K. Heinemann, President and Grant Administrator
William C. Pitts, Principal Investigator
17 December, 1991

INTRODUCTION

Spacecraft entering a planetary atmosphere require a very sophisticated thermal protection system. The detail design must be tailored to each specific vehicle based on its planned mission profiles. For the Space Shuttle several types of ceramic heat shield insulation materials were developed, both flexible and rigid. These worked very well. Future entry spacecraft will have even more stringent requirements on the thermal insulations. To be prepared for this need, the staff of the Thermal Protection Materials Branch at NASA Ames continues to improve the old materials and to develop new materials (Refs. 1,2,3 and 4). Among the goals of this effort is the development of insulation materials with higher temperature limits, material strength, and surface ruggedness; to reduce weight; and to reduce surface catalycity. Having developed these materials, their thermal performance capability must be compared with that of other insulation materials. Also, the ability of the new materials to provide thermal protection for proposed spacecraft must be evaluated. This is done both experimentally and by numerical analysis. This report presents a summary of the results of a series of such calculations performed between August 1986 and July 1991.

TOPHAT, AN IMPACT RESISTANT TILE INSULATION

A shortcoming of the rigid, Reusable Insulation (RSI) tiles used on the Space Shuttle is that the black reaction cured glass (RCG) coating was very fragile. It is important that the heat shields for future spacecraft be resistant to

surface impacts. A rigid surface, heat shield tile design, called Tophat, was proposed by Riccitiello in Ref. 5 of. The tile consists of a low-density rigid ceramic tile covered by a silicon-carbide cover that slips over the ceramic tile. The rigid cover adds weight to the tile so a portion of the rigid tile is hollowed out and replaced with a lower density ceramic. To be useful this tile must also be weight competitive with other ceramic tiles. As part of the current program an analysis was made to show that it can be. The procedure and results of this analysis are presented in Ref. 5. It is shown that a thermal protection system using tophat tiles is 10% heavier than a system using Fibrous Refractory Composite Insulation, FRCI. The percentage weight difference diminishes as the heat load increases. Even though there is some weight penalty for the Tophat surface relative to the Shuttle tile, FRCI, the penalty may be acceptable in exchange for a more durable insulation.

Development of this Tophat concept is continuing.

CATALYTIC SURFACE

Flight tests on the Space Shuttle (Ref. 2) have dramatically demonstrated the effect of surface catalycity on the local heat transfer rate to the RCG coating on the RSI tile surfaces. This catalycity effect has not been so obvious in arc-jet test data, but was noted in a recent arc-jet test conducted by Wendell Love of the Ames Research Center. He observed a significant temperature increase when he painted the surface of a low catalycity graphite, wing leading edge model with a highly catalytic material. An analysis was undertaken to quantify the magnitude of this catalytic effect.

The analysis was done using a two-dimensional numerical model developed specifically for this analysis. This model was designed to give the net heat flux to the model surface using the measured temperature history as the boundary condition. The basic element in this analytical model is the heat balance equation for a typical surface element.

$$Q_{in} = \sigma \epsilon_s A_s T_s^4 + \rho V C_p \Delta T + \sum_n k_n (T_n - T)$$

The first term is the reradiation from the surface, s. The second term is the heat absorbed by the surface element. The third term is the sum of the heat conduction terms to adjacent elements. The model also included conduction exchange between all adjacent inner elements. Using the measured values for T_s as a boundary condition, the heat flux history was calculated for model runs with and without a catalytic coating on the model, but with the same arc flow conditions. The ratio of the heat flux with the catalytic coating to that without gives a measure of the catalytic effectiveness of the coating. There were two major deficiencies in knowledge about the models. One was the exact depth of the thermocouple (about .040 inch), and the other was the conductivity of the model material. The material was graphite, but handbooks show a fairly wide range in magnitude of thermal conductivity. All data show the same significant variation of conductivity with temperature. For this analysis it was assumed that because these uncertainties were the same for both models, the ratio of the heat fluxes for the two models would not be significantly affected. Subsequent sensitivity checks verify this. It was found that the use of a constant average thermal conductivity gave the unrealistic result that the arc flow

enthalpy increased steadily with time although the arc parameters were all steady. Use of proper temperature dependent conductivities corrected this problem. The results of the analysis are tabulated in the following table: (Results are averages for the portion of the data between 8 and 30 seconds. Prior to this time the arc starting transients cause problems. After this time the catalytic coating erosion was likely to be significant)

Analytical Model	Ratio of Heat Fluxes	
	Stagnation	Side
Nominal	1.37 +/- .04	1.27 +/- .04
Nominal but 1/2 Conductivity	1.38 +/- .04	1.30 +/- .04
Nominal but depth adjusted	1.41 +/- .04	1.28 +/- .04
1-dimensional approximation	1.52 +/- .10	1.60 +/- .08

It is apparent that the catalytic paint increased the heat flux to the stagnation region about 40% and to the side surface about 30%. This trend along the surface is as expected . As assumed, the ratioed results are insensitive to conductivity and to thermocouple depth. The absolute values for heat flux are very sensitive to these parameters, but the magnitudes fall within the expected range for the arc-jet test conditions. It is apparent that a one-dimensional model is not adequate. The ratio values for the 1-D model differ from those using the 2-D model and the expected trend of decreasing catalytic effect along the surface is reversed. These results were presented in Reference 6.

LH2 FUEL TANK INSULATION

Many future spacecraft will use liquid hydrogen for fuel. These fuel tanks must be well insulated to minimize boil off due to aerodynamic heating during the ascent and descent phases of the missions. For all spacecraft, there will be

competing options for the thermal protection material used. A preliminary comparison is made here of the performance of two types of insulation for the cryogenic fuel tank for a typical vehicle and mission. One is the flexible ceramic fiber insulation, Tailorable Advanced Blanket Insulation, TABI and the other is a multilayer insulation, MLI. TABI is a flexible ceramic blanket that is an evolution of the flexible ceramic blankets that were used successfully on the upper surfaces of the Space Shuttle. MLI is a multi layered blanket of thin metal foils separated by an open mesh cloth or by dimples in the foil. The MLI is covered top and bottom with a ceramic fabric. In lieu of detailed information on the design of the tank walls, both insulation systems for the analytical model are fastened directly to a simple aluminum wall tank with RTV. The cryogenic is treated as a constant temperature heat sink. The heat transferred into the tank is accomodated by cryogenic boiloff. The criterion for comparison of the two insulation systems is the relative weights when the same amount of heat is transferred into the tank under identical heating conditions. Although simplified, these models should provide a reasonable first cut performance comparison between the two systems.

The heating environment imposed on the two systems is based on the the stagnation point heating rates calculated for a proposed National Aerospace Space Plane (NASP) mission. The flux to the tanks will of course be much less than this so calculations were made using fluxes that were 1 and 10 percent of the stagnation point values. The computer models are one-dimensional. The temperature dependent properties of AFRSI at .01 atm are used for the

ceramic insulation, but because the Shuttle type ceramic insulations have similar thermal conductivities, the results will be representative of all of them. Because the mission altitude ranges from ground level to maximum mission altitude, the pressure dependency of the conductivity should be included. This can be entered in the next phase. The MLI is treated as providing an effective emittance between the inner surface of the cover plate and the outer surface of the tank wall.This is common in the analysis of thermal control systems using MLI. A series of calculations was made of the total heat flux into the tank with varying thickness for the ceramic insulation and with varying effective emissivity for the MLI model. The results of these calculations are summarized in Figure 1 for 1% and 10% of the stagnation point heating level. The two systems are thermally equivalent if they allow the same total heat load to the tank during the mission. The figure shows the insulation surface density for the two insulation systems for both heating rate profiles for a range of acceptable heat loads. It is apparent that for the models and assumptions of this preliminary analysis, the TABI system is generally the lightest. (An advanced, lighter weight MLI design, discussed later, would affect this conclusion). For low heat loads into the tanks the MLI system can be the lightest. This may be achieved by adding a high temperature thermal protection system above the MLI component. MLI may also be competitive on the lee side of the vehicle where heat loads are small. For reference: 1 kJ of heat will boil about 2 grams of LH2 at 1 atm. and the heat capacity of LH2 is about 1 joule/gm/K. These results were presented in Reference 6.

PHASE CHANGE MATERIAL TO COOL NASP TANKS

Another concept for insulating the NASP LH2 tank was suggested by Howard Goldstein of NASA Ames. He suggested the use of a layer of a metal hydride on the LH2 tank wall where it would serve both as a structural component and as a phase change material, PCM. This could be very desirable because the heat protection mechanism would be operating directly on the fuel tank. A quick look was made of the feasibility of using this concept.

For this application, hydrogen, stored within the hydride would be released endothermically as the hydride reaches its critical temperature range, thus maintaining the hydride temperature until all of the hydride has decomposed. Although the concept of using metal hydrides in spacecraft fuel tank insulation systems is apparently new, metal hydrides have been suggested for storage of hydrogen for land based fuel cells, Ref. 7. The basic concept of storing hydrogen in a hydride is discussed there and shown in Figure 2. There the dissociation pressure is shown as a function of the hydrogen composition within a typical hydride. The temperature remains relatively constant as the hydride dissociates from maximum hydrogen concentration to nearly zero concentration. The temperature depends on the dissociation pressure. This reaction is reversible and generally without hysterisis. The numerous hydrides that exist provide a wide range of numbers that go with this typical curve form as well as a wide range of heats of formation.

The procedure followed in this analysis was to make parametric calculations to establish the range of numbers for Figure 2 that are required for a PCM to be effective.

Then a search was made for a metal hydride that satisfied the requirements. Practical problems such as the strength requirements for the hydride are not within the scope of this preliminary analysis. It was assumed that the weight of the fuel tank was the same whether or not it was partially composed of a hydride.

This analysis was made using a simple one-dimensional model, Figure 3. The insulation material used outside the metal hydride PCM is LI-900. A liquid hydrogen compatible foam is used inside the PCM. The foam is lined on the inside with an aluminum shell. The total insulation thickness (LI-900 plus foam) is varied in the analysis as well as their relative thicknesses. The PCM transition temperature and the dissociation heat capacity of the PCM are also varied.

A special one-dimension, transient heat-flow computer code was written for this analysis. The temperature dependant thermal conductivity of LI-900 was accounted for. For simplicity of the comparative analysis, the physical and thermal properties of the foam were assumed to be the same as those of the LI-900. The basis of comparison for the various combinations of these parameters was the integrated heat flow through the aluminum liner while exposed to a typical heat flux profile for a NASP flying a cruise trajectory.

The dependence of liquid hydrogen boiloff weight on total insulation thickness is shown in Figure 4. The lower pair of curves are for LI-900 insulation with and without PCM included. For both cases, the optimum insulation thickness is between 0.7 and 0.8 inch. The use of the PCM reduces the minimum weight of insulation plus boiloff LH2 by about 20% for this case. Most of this weight reduction is in the amount of LH2 boiled off,

and because the weight of the two components are comparable, this means that the boiloff weight is reduced by almost 40%. The upper pair of curves show the corresponding result for LI-2200 insulation. The total weight saving is again about 20%, but because of the higher density of LI-2200 (22 lb/ft^3 instead of 9 lb/ft^3) the optimum insulation thickness is smaller and the amount of LH2 boiled off is larger.

The results shown in Figure 4 were for cases with the PCM at a depth of 1/4 of the total thickness of the insulation and foam, with the transition temperature at 125 F, and with the heat absorbing capacity of the decomposing hydride equivalent to a 0.4 inch sheet of water ice. The performance of the PCM depends on all of these quantities. Some insight on how is shown in Figure 5. The curves show the heat fluxes to the aluminum liner of the tank as a function of time. The solid curve is for the case of no PCM. When the PCM is at a depth of 0.5 of the thickness, it is not very effective. For one thing, it takes longer for the temperature to reach the transitional level. The major effect, though, is that the transition temperature is fixed at a level closer to the liner than it is for the 0.25 inch depth case. Thus the thermal gradient at the liner is larger. For the 0.5 level not all of the 0.4 inch equivalent ice heat absorbing capacity is utilized. At the 0.25 level, it is used up near the end of ascent. For half this capacity, the hydride is fully decomposed early in the ascent. When it is, the heat flux rises rapidly to the no PCM levels. The effect of transition temperature would appear the same on this figure as does the effect of PCM depth.

The effect of PCM depth is shown in more detail in

Figure 6. The minimum weights were determined from curves similar to those of Figure 4. As indicated by Figure 5 the optimum depth is dependent on the available heat absorbing capacity. It is apparent that for all cases, the PCM should be placed relatively near the surface for maximum benefit. The higher the available heat capacity, the closer the PCM should be placed to the surface. This trend is almost linear as shown by Figure 7.

A typical trend of minimum weight with the transition temperature is shown in Figure 8. It is apparent that a low transition temperature is desirable. However, this trend is limited by the fact that the PCM would decompose in the prelaunch environment if the transition temperature was too low. At the high end of the scale the PCM is ineffective because the transition temperature is not reached until well into the ascent unless the PCM is placed close to the surface. Then, unless the absorbtion capacity is very large, the hydride temperature limit will be exceeded when the decomposition is completed.

The foregoing results were selected from a set of calculations in which the pertinent parameters were systematically varied. The maximum weight reduction due to the use of PCM was found to be about 25%. For this case the PCM was 0.14 deep within the insulation, the transition temperature was 125 F, and the heat absorbtion capacity was equivalent to 0.8 inch of ice. This is not a desirable design because the heat absorbtion requirement is so large and the tank structure is dangerously close to the surface, but it does indicate the maximum benefit attainable for this type of heat protection system.

The final step of this study was to search the literature for the best metal hydride to match the indicated requirements. These requirements are: a large heat absorbtion capacity, a low transition temperature, a high rate of dissociation, stability in the prelaunch environments, and suitable structural characteristics. Unfortunately, most of the work on the use of metal hydrides for hydrogen storage has been directed toward fuel cell applications where a low heat absorbtion capacity and a high transition temperature is desired (Ref. 7). There are many binary and ternary hydrides with a wide range of characteristics. These characteristics can be varied substantially by the the addition of impurities.

The two most likely candidates found were MgNi-H and FeTiH. They both have low transition temperatures and high rates of decomposition. Both have a high storage capacity for hydrogen on a volume basis, but because of the high densities of the metal component, their capacity on a weight basis is reduced to near that of water. The capacity of MgNi-H is about 10% higher than water and that of FeTi-H is about 40% lower. There is also a question of the stability of these hydrides in the vacuum of space.

Conclusion: The analysis on the feasibility for using metal hydrides in the thermal protection system of cryogenic tanks in space was based on the heat capacity of ice as the PCM. It was found that with ice the thermal protection system weight could be reduced by, at most, about 20 per cent over an all LI-900 insulation. For this concept to be viable, a metal hydride with considerably more capacity than water would be required. None were found. Special metal hydrides were developed for hydrogen fuel storage applications and it may be

possible to do so for the current application. Until this appears promising further effort on this feasibility study does not seem warranted.

The results of this analysis were presented in Reference 8.

COMPOSITE FLEXIBLE BLANKET INSULATION

Flexible, ceramic blanket insulations, have been used very successfully in a variety of forms to protect the Space Shuttle from the heat generated by atmospheric entry. Multi-Layer Insulation, MLI, is a standard form of insulation for the thermal control of spacecraft while in the hard vacuum of space. H. E. Goldstein of NASA Ames Research Center (private communication) has suggested the possibility of combining these two types of insulation into a composite insulation system for the thermal protection of advanced spacecraft during atmospheric entry.

A developmental task was undertaken by Kourtides, Pitts, et al (Ref. 9) to demonstrate that a ceramic flexible blanket insulation, CFBI, with MLI stitched to the lower surface could be fabricated and tested.

The insulations consist of ceramic fabrics, insulations, stainless steel foils, and skrim cloth spacers all quilted together using ceramic thread. Silica and three types of aluminoborosilicate (ABS) were considered as options for the skrim cloth. These materials and the stainless steel foil were chosen because they were readily available and because they were reasonable materials for a feasibility study rather than a result of an optimization study. These materials were successfully fabricated into the desired insulation blanket form and tested to determine their performance characteristics.

The data were correlated using a one-dimensional numerical model. The correlation showed that the MLI component of the insulation blanket had an effective conductivity close to that of air at 1 atmosphere pressure. This is reasonable because for continuum flow, which it still is at the test pressure of20 mm Hg, the conductivity of air is independent of the pressure, and at the foil temperatures of the test, thermal radiation is negligible compared to the heat transfer through the air between the foils. At high altitudes, where the flow approaches free molecular, the conductivity of air diminishes linearly with the pressure. For the AFE, the entry heating takes place above 250,000 feet. There the mean free path is greater than 0.1 inch compared to a foil spacing less than 0.01 inch so that the flow within the MLI would be free molecular.

There was no effort to optimize the MLI design and the tests run on the samples did not adequately simulate the space environment. Consequently, it was difficult to estimate from the results of this program the potential weight benefit to be gained by using this type of system. To make such an estimate, a numerical analysis was performed using the concept of Reference 9, but with improved weight characteristics. This analysis was also directed to a concern for the Aeroassist Flight Experiment (AFE) mission to be flown by NASA (Ref. 10). This concern is that the RTV used to bond the thermal protection system to the vehicle skin will outgas when heated and contaminate the windows of radiometers on board. Therefore, it may be necessary to keep the RTV peak temperature well below its normal limit.

The present analysis showed that the stainless steel

foils and skrim cloth to separate the foil layers are too heavy to be weight competitive with just a ceramic blanket insulation. Therefore, for this numerical analysis, the foils were replaced with 0.00025 inch thick aluminum foils and the skrim cloth was replaced with a thin, very loose weave silica cloth. The chosen MLI consists of 10 alternating layers of these materials with a combined weight of 0.04 lbm/ft^2. The outer foil temperatures will exceed the usual structure limits for aluminum, but they carry no loads so this will not be a problem. For this analysis the lower fabric of the blanket was assumed to be bonded to the aluminum skin of the AFE by a 0.01 inch thick layer of RTV. It is the prescribed temperature limit of this RTV that is the criterion for selecting the required insulation thickness.

The numerical program used was written especially for this analysis. The model is one dimensional. The prescribed heat flux is imposed on the front surface. Heat is reradiated to space from the front surface and conducted inwardly through the silica felt and MLI to the RTV and aluminum skin. Radiation between the aluminum foils is also accounted for. The inner surface of the vehicle skin interacts radiatively with the AFE structure which is assumed to be at a fixed temperature. The temperature dependant conductivities and heat capacities of the materials are accounted for. The numerical analysis proceeds in a stepwise fashion using a relaxation technique.

The procedure is to calculate the RTV temperature as a function of time during the entry maneuver to determine its peak value for a variety of parameters. The primary parameters considered were the effective conductivity between

foil layers, the thickness of the silica felt component, and the number of layers of foil in the MLI. From these calculated results the silca felt thickness required to meet the RTV temperature criteria were determined and weight comparisons were made.

The basic and most interesting results are summarized in Figure 9. The peak RTV temperature is shown as a function of silica felt thickness. The MLI component thickness is in addition to this. The upper curve represents the case for no MLI. The other curves represent cases with MLI included. These curves assume different, effective conductivities between the foil layers due to conduction through the gas, skrim cloth, and the stitches. The conductivities are related to the conductivity of standard air because this was approximately the MLI conductivity exhibited by the test data presented in Reference 9. Conductivities less than this should be easily achieved because no effort was made to optimize the skrim cloth used, and because the gas conductivity will be much less in the free molecular flow environment at entry altitudes.

From these curves, the felt thicknesses required to limit the RTV temperatures to 250 F, 300 F, and 400 F were determined. The CFBI weights for these thicknesses are presented in the following table which shows the heatshield weights, in lbm/ft^2, for several MLI conductivities, k

RTV Temperature, F	No MLI	With MLI		
		k = 1.	k = .5	k = .2
250	.37	.30	.21	.10
300	.28	.21	.13	.10
400	.18	.10	.10	.10

The minimum thickness allowed for the silica felt was 0.1 inch because it would be difficult to fabricate the blanket if thinner than this.

It is apparent that there is significant potential benefit to be gained by using CFBI. Weight savings of the order of 0.2 lbm/ft^2 are indicated. Considering the large area of spacecraft this would amount to a sizeable weight saving. More results are presented if Reference 11. In view of the preceding calculations, the physical development of CFBI was continued with emphasis on reducing the weight of the insulation system. The stainless steel foils were replaced by aluminum and aluminized polyimide foils. The weight of the skrim cloth that separates the foils was reduced, in the case of the aluminized polyimide foils, the option of not using a skrim cloth was examined.

The thermal performance data show that for all of the ten samples fabricated the overall thermal conductivity of the composite is significantly lower than that of the ceramic blanket alone. Analysis of the data shows that for the best of the options, the effective conductivity of the MLI component is about 60% of the ceramic blanket component it replaces. These results are presented in detail in Reference 12.

CERAMIC MATRIX COMPOSITE PROGRAM

There is a need for oxidation resistant insulation materials that can perform at temperatures higher than those developed for the Space Shuttle. The material must also be tough enough to survive the handling and operational environment. Fiber reinforced ceramic matrix composite materials are candidates to meet these requirements. After examination of several possibilities SiC fibers emerged as

the most likely material to examine in detail.

A major problem is the creation of a strong bond between the SiC fiber and matrix without seriously damaging the fibers. Standard ceramic processes are unacceptable. Insitu formation of SiC from precursor chemicals using chemical vapor infiltration (CVI) offers a promising approach to the problem. This procedure has been examined using an induction heated furnace provided by NASA. The research focused on SiC for the matrix produced by the thermal decomposition of dimethyl-dichlorosilane, and Nicalon plain weave fabric as the SiC fiber source. Several methods of introducing the reactant gases to the laminate were considered as well as the effect of several process variables. It was determined that a modified diffusion process provided the best method of introducing the reactant gases. The infiltration conditions that were found to produce the best results were: 900 C temperature, 5 torr pressure, 2.9% (vol.) reactant concentration, using hYdrogen as the carrier gas.

Using these conditions, a preliminary sample of SiC/SiC composite was manufactured. The total run time required for its fabrication was 125 hours. This composite had a fiber density of about 35% and was about 75% dense. Although the strength of the specimen does not meet the desired goal, its flexural strength greatly exceeds that of a C/SiC composite, and it is about 2.5 times stronger than 80% dense reaction bonded, monolithic SiC. The details of this development procedure are presented in Reference 13.

INFLATABLE DECELERATOR

Several types of inflatable and expandable decelerator have been proposed for atmosphere entry (Refs. 14 and 15).

For these applications, some form of flexible, insulating fabric with a back surface stiffener has generally been proposed. An alternate approach for single entry vehicles would be to put the stiffening material on the front surface where it would serve as an ablating surface. A brief analysis was made for this type of system that shows that it does have a potentially significant benefit.

For the analysis, a one-dimensional thermal conduction model was programed. Nextel was used for the fabric and RTV 325 was used for the ablation material. The thermal properties for the Nextel were assumed to be the same as those of AFRSI at .01 atmosphere (Ref. 1). RTV 325 is the most suitable of the available RTV's for a thermal protection ablator. A value of 5000 Btu/lb was used for the effective heat of ablation for the RTV at an effective temperature of ablation of 900 F. The front surface heat flux imposed on the model is shown in Figure 10. A back surface temperature limit of 600 F was assumed for the comparative analysis between the Nextel/RTV combination and a plain Nextel blanket.

The results of the analysis are summarized in the following table showing the decelerator material thickness requirements.

MATERIAL	THICKNESS (inch)	SURFACE DENSITY (lbm/ft2)
Nextel	.30	.18
Nextel/RTV	.10	.10

These thicknesses were determined from the analysis to limit the back face temperature to the assumed limit of 600 F. For application to a spacecraft a margin of safety should be added to the thickness of both systems. It is apparent that the use of the RTV ablator provides a significant weight

benefit for this case and should be considered for any future spacecraft which requires only a one time use of its thermal protection system.

PERSONNEL LAUNCH SYSTEM

The Space Station Freedom will require more personnel transfer capability to and from earth than the Space Shuttle manifest can accommodate. To supplement the Shuttle, Personnel at the NASA Langley Research Center are conducting definition studies of a Personnel Launch System (PLS). It is a lifting body design with a moderate lift to drag ratio. It will require a thermal protection system to protect it from aerodynamic heating during earth atmosphere entry. The results of a study in which ceramic insulations are used for such a system are presented in Reference 16. These results are summarized below.

LI900 and AFRSI (Advanced Flexible Reusable Surface Insulation) were respectively the first rigid and flexible ceramic insulations developed for the Space Shuttle. Subsequently other ceramic insulations have been developed for Shuttle application and for advanced spacecraft. The rigid insulations include FRCI (Fibrous Refractory Composite Insulation) and AETB (Alumina Enhanced Thermal Barrier). The flexible insulations include TABI (Tailorable Advanced Blanket Insulation) and CFBI (Composite Flexible Blanket Insulation).

The primary purpose of this study was to compare the capabilities of all of these materials for the thermal protection of the Personnel Launch System. An ancillary purpose was to examine the differences between the TPS requirements for aluminum and for graphite-polyimide

surface structures (graphite polyimide is baseline for the PLS windward surface). It was found that for this mission, the ceramic insulations can be used over nearly all of the vehicle surface. On the leeward surfaces the flexible materials are preferred because they require less weight and are easier to apply. Because so little insulation is required there, no significant weight advantage was found among the various blanket materials. On the windward surfaces the rigid tiles are preferred because the blanket materials are more vulnerable to aerodynamic loads and acoustics. Otherwise, state of the art TABI might be considered for the wing lower surface on the basis of a significantly lower weight relative to the tiles. Encouraging, unpublished data on an improved version of TABI suggest that CFBI with a TABI surface has the potential to flight qualify and provide the lightest TPS here. Along the centerline, AETB8, AETB12 and FRCI12 are all candidate materials. The calculated insulation thicknesses and TPS surface densities are comparable to those of the Space Shuttle. The AETB8 TPS is significantly lighter than the others, but the choice will depend on flight durability factors. The required local insulation weight is on the average 30% lower for the graphite-polyimide than for the aluminum surface structure. Determination of the total system weight requires the calculation of the two surface structure weights which is beyond the scope of this study.

The details of this study are presented in Reference 16.

MESUR PROBE AEROBRAKE

NASA is conducting a preliminary design study of a probe to enter the Mars atmosphere and make in situ measurements of

the environment. A major part of this study is the selection of a thermal protection system for the probe as it enters the atmosphere in an aerobrake mode. The Eloret staff was asked to participate in this selection process. The results of this effort are described in Reference 17.

Two entry velocities were considered, 7 km/sec and 9 km/sec. For the former the peak heat flux to the surface is only about 75 W/cm^2 so a non ablating heat shield is possible. For the latter the heat flux approaches 200 W/cm^2 so that an ablating heatshield is required. The work reported herein was focused primarily on the nonablating case. For this case the peak surface temperature was estimated to be about 3000 F if the worst case assumption of a fully catalytic surface is made. This temperature is a little higher than the recommended maximum temperature for the Space Shuttle type reuseable surface insulation, RSI, tiles. However, even a fraction of the catalyticity reduction observed for the Shuttle tiles during entry would reduce the surface temperatures to an acceptable level. The concern is that the Mars atmosphere is predominantly CO_2 and the catalytic effect in CO_2 has not been well established. Nevertheless, a calculation was made to determine the thickness requirement of a Shuttle type tile. Alumina Enhanced Thermal Barrier, AETB12, was selected because it is the toughest of the available silica tiles, and it offers the best resistance to the expected sand erosion environment. It was found that the minimum manufacturable thickness of AETB12 was more than sufficient to maintain the aluminum aerobrake skin temperature to less than the 350 F limit. A second alternative material considered was SLA-561, an elastomeric silicone material

manufactured by Martin Marieta Corp. This material was used for the heat shield material on the Viking mission to Mars. Calculations were made both as a nonablator and as a pyrolizing ablator. The two calculations produced nearly the same thickness requirements. The factoring of this information together with other design requirements provided by other investigators is discussed in Reference 17.

REFERENCES

1. Goldstein, H. E., "Fibrous Ceramic Insulation," NASA CP 2251, Nov. 1982.

2. Stewart, D. A., Rakich, J. V. and Lanfranco, M. J., "Catalytic Surface Effects on Space Shuttle Thermal Protection System During Earth Entry of Flights STS-2 Through STS-5", NASA CP 2283, March 1983.

3. Sawko, P. M., "Tailorable Advanced Blanket Insulation," Proceedings of Fiber-Tex Conference sponsored by NASA and Clemson University, Clemson, South Carolina, Nov. 1987.

4. Leiser, D. B., "Space Vehicle Thermal Protection," Alumina Chemicals: Science and Technology Handbook, edited by L. D. Hart, The American Ceramic Society, 1989.

5. Riccitiello, S. R., Pitts, W. C., Smith, M. and Zimmerman, N. B., "Toughened Outer Surface Reusable Surface Insulation for Advanced Thermal Protection Systems", Draft of proposed paper for AIAA Journal of Spacecraft and Rockets, (Submitted with Semiannual Report for NASA Cooperative Agreement NCC2-434 dated April 4, 1987.

6. Semiannual Report for NASA Cooperative Agreement NCC2-434 dated April 4,1987.

7. Hydrogen: Its Technology and Implications, Volume II, Transition and Storage, Chemical Rubber Company Press, 1977.

8. Semiannual Report for NASA Cooperative Agreement NCC2-434 dated October 30, 1987.

9. Kourtides, D. A., Pitts, W. C., Araujo, M., and Zimmerman, R. S., "High Temperature Properties of Ceramic Fibers and Insulation for Thermal Protection of Atmospheric Entry and Hypersonic Cruise Vehicles," Jan. 1988. (Submitted with Semiannual Report for NASA Cooperative Agreement NCC2-434 dated November 2, 1989.

10. NASA-MFSC FY 1986 AFE Definition Review Report, May 1986.

11. Pitts, W C and Kourtides, D A, "Ceramic Insulation/ Multifoil composite for Thermal Protection of Reentry Spacecraft,"

AIAA Paper 89-1772, June 1989. (Submitted with Semiannual Report for NASA Cooperative Agreement NCC2-434 dated November 2, 1989.

12. Kourtides, D. A., and Pitts, W. C., " Composite Multilayer Insulations for Thermal Protection of Aerospace Vehicles," Paper presented at the "Composites in Manufacturing 8" Exposition and Conference, Society of Manufacturing Engineers, Anaheim, CA, Jan 1989. (Submitted with Semiannual Report for NASA Cooperative Agreement NCC2-434 dated January 30, 1989.

13. Carswell, M. G. and Riccitiello, S. R., "Silicon Carbide Matrix Composites Produced by the Thermal Decomposition of Dimethyldichlorosilane", NASA TM 102881, January 1991.

14. Walberg, G. D., "A Survey of Aeroassisted Orbit Transfer," AIAA Paper 82-137, Aug. 1982.

15. Menees, G. P., :"Trajectory Analysis of Radiative Heating for Planetary Missions with Aerobraking of Spacecraft," AIAA Paper 83-407, Jan. 1983.

16. Chiu, S. A. and Pitts, W. C., "Reusable Surface Insulations for Reentry Spacecraft", AIAA Paper 91-0695, January 1991. (Submitted with Semiannual Report for NASA Cooperative Agreement NCC2-434 dated January 14, 1991.

17. Tauber, M. E., "MESUR Probe Aerobrake Preliminary Design Study - Appendix A", September 30, 1991.

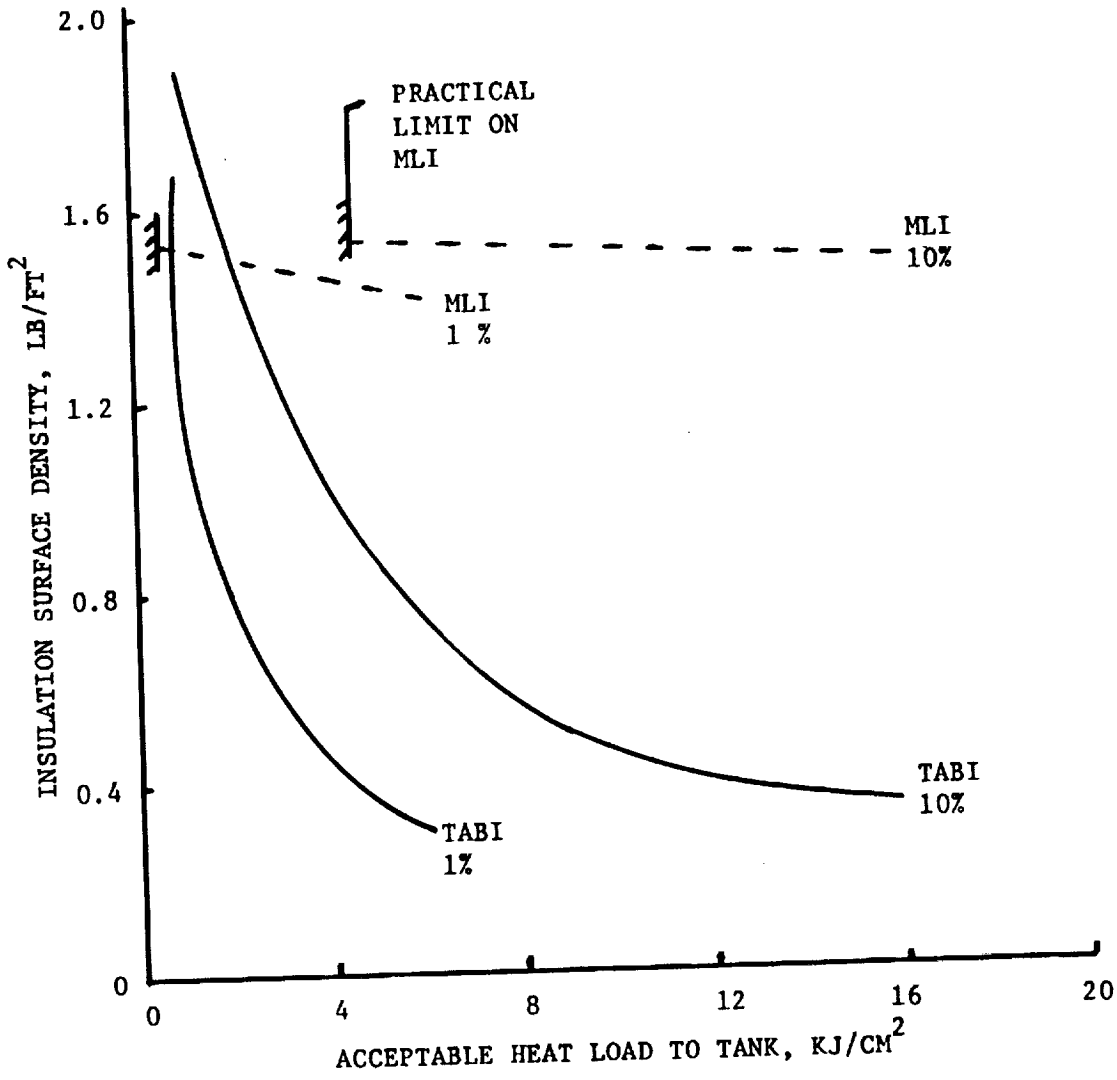

Fig. 1 Weight comparison between MLI and TABI for same heat load to tank.

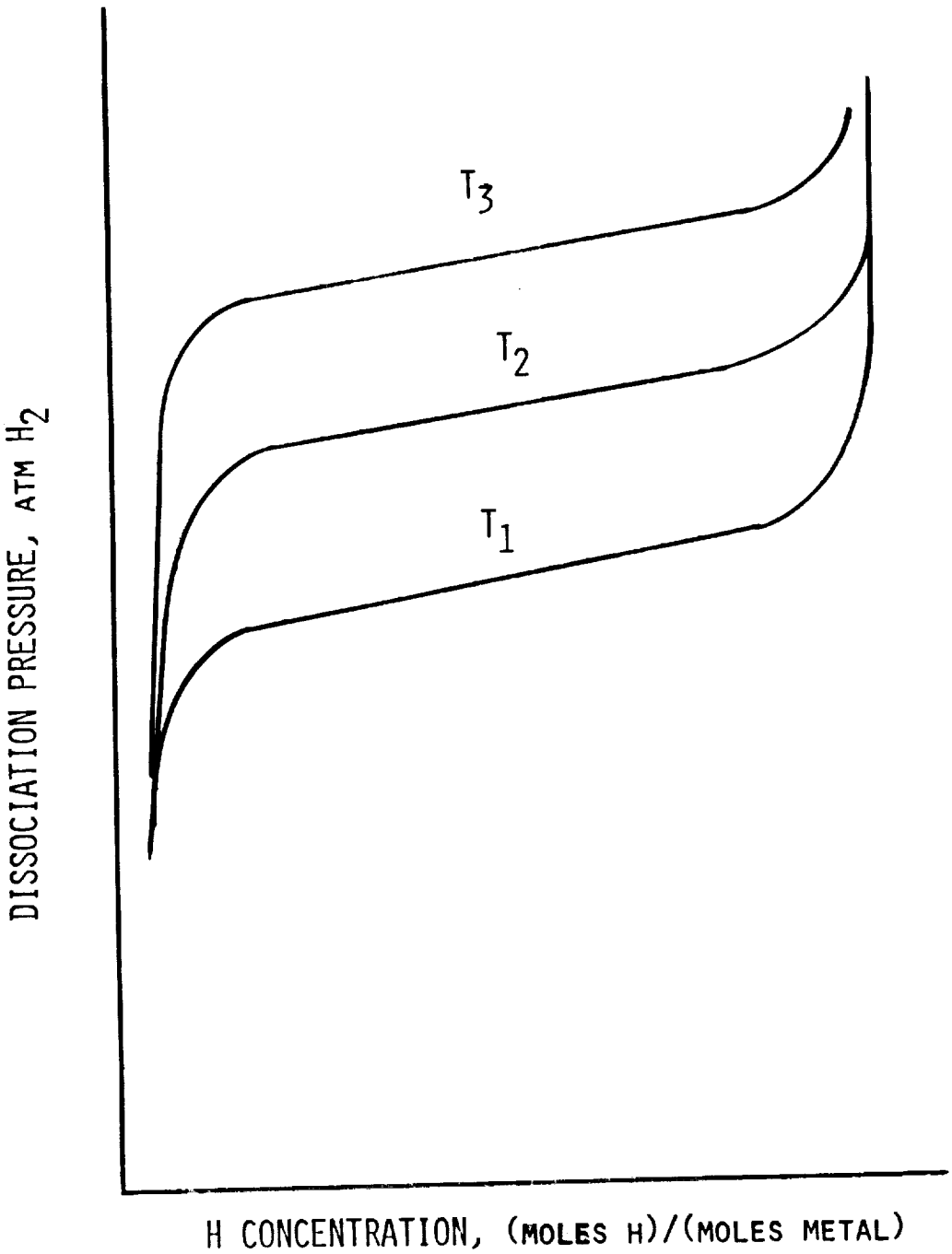

Figure 2 . Phase change diagram for metal hydrides.

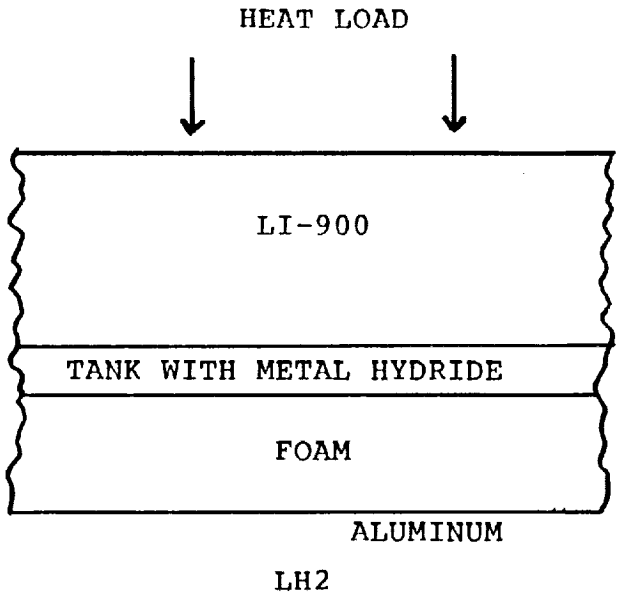

Figure 3. One dimensional model used for analysis.

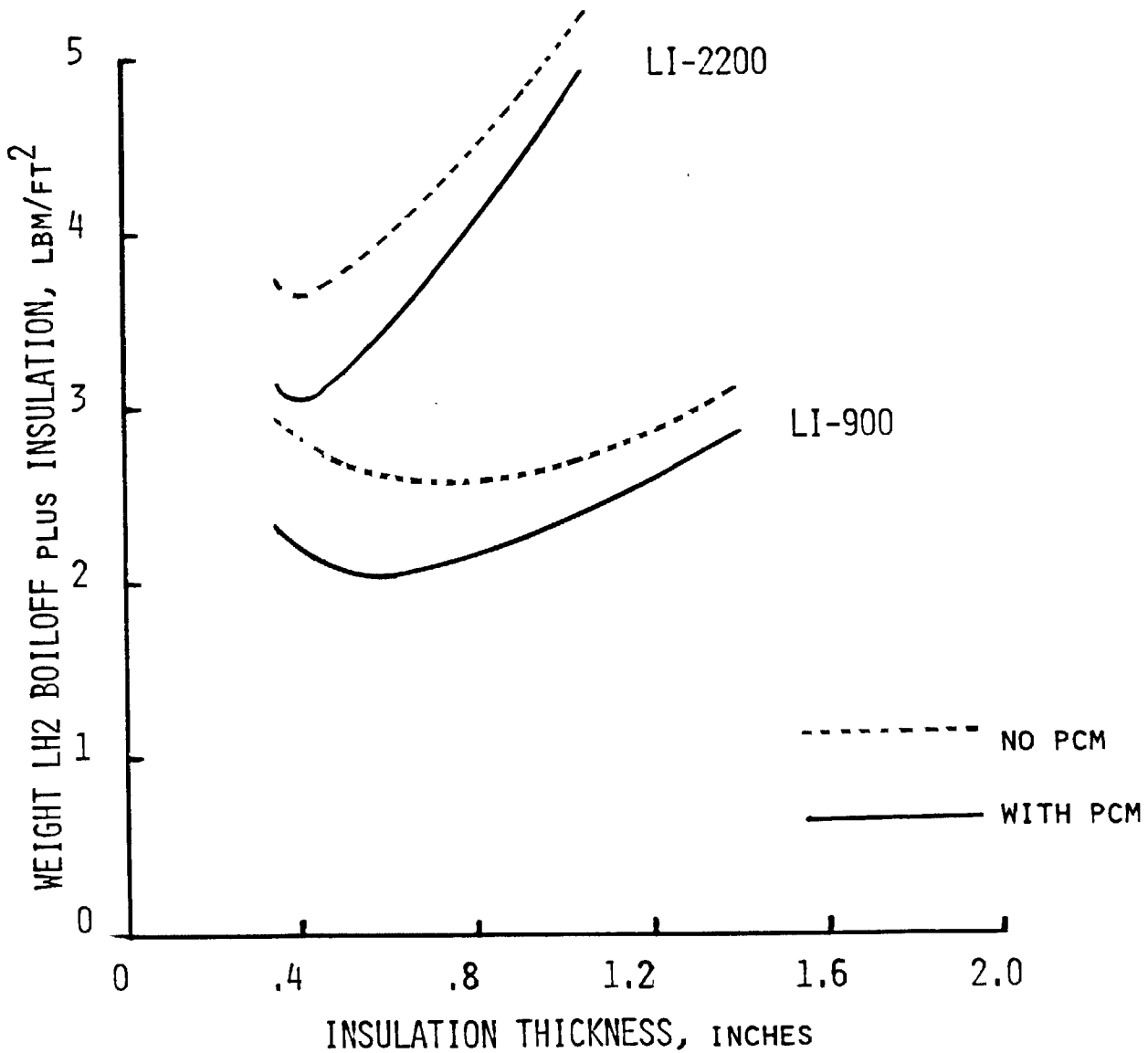

Figure 4. Effectiveness of metal hydride PCM as a thermal protection system component.

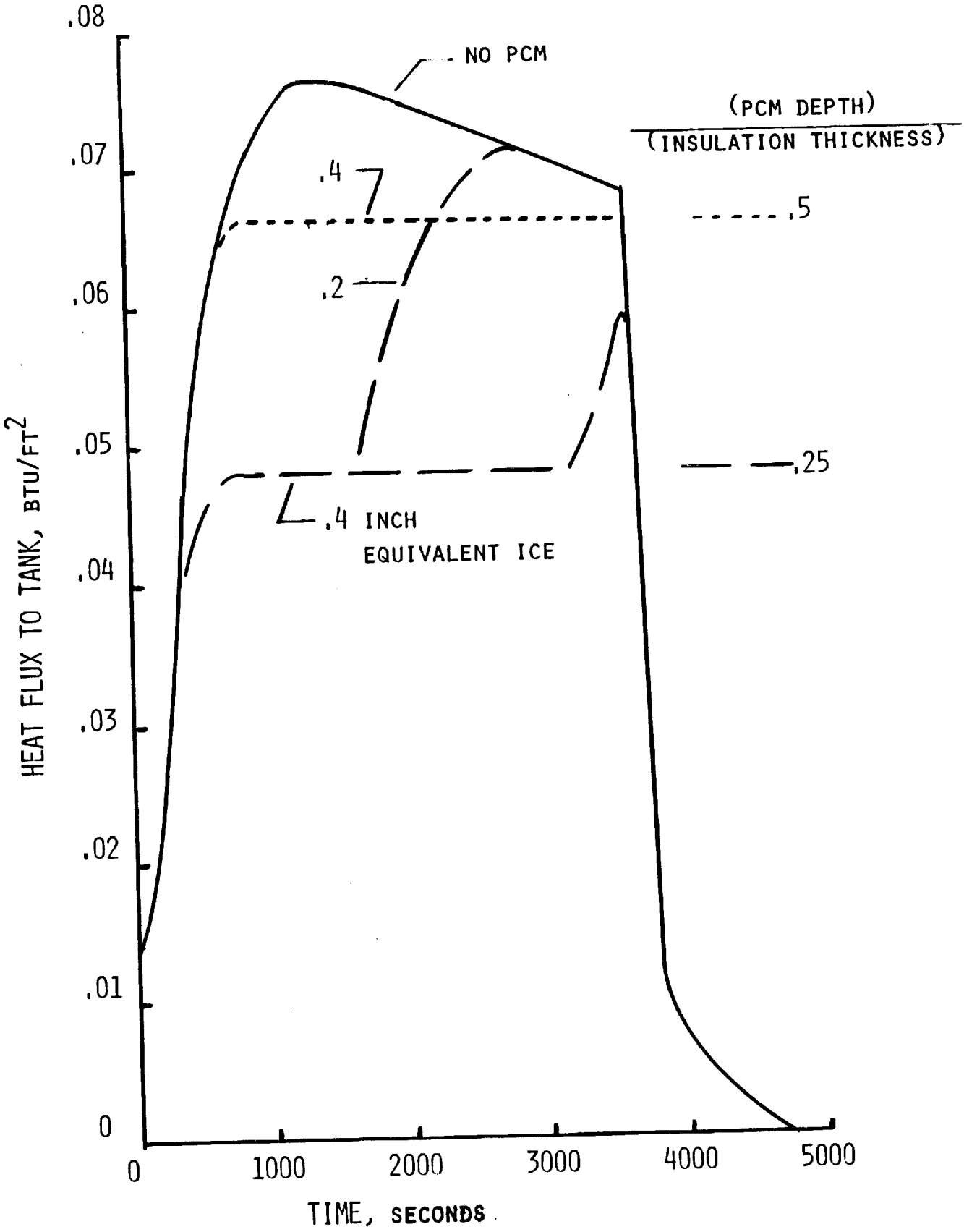

Figure 5. Dependence of heat flux to tank on model parameters.

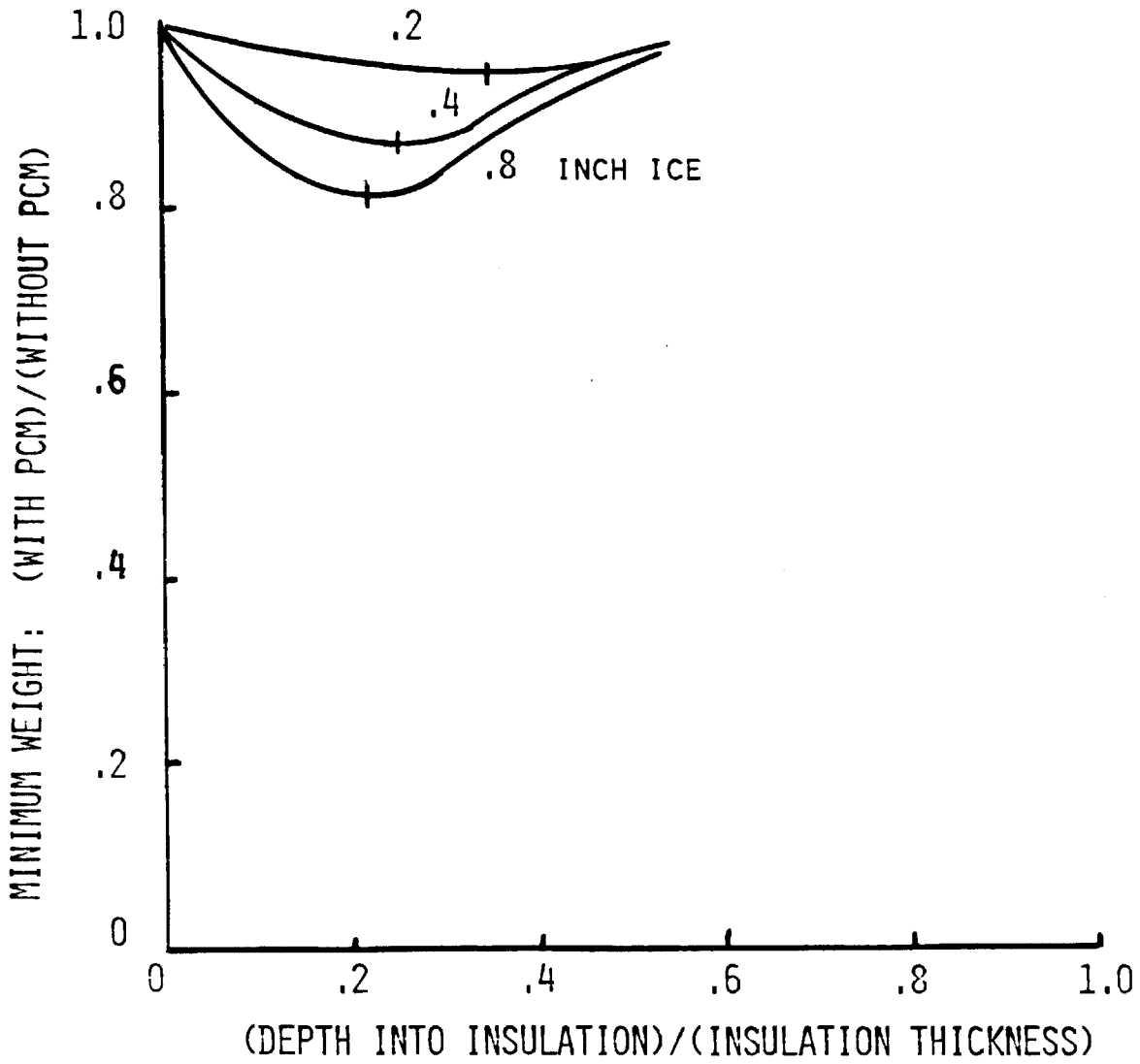

Figure 6. Dependence of minimum weight on depth of PCM within insulation.

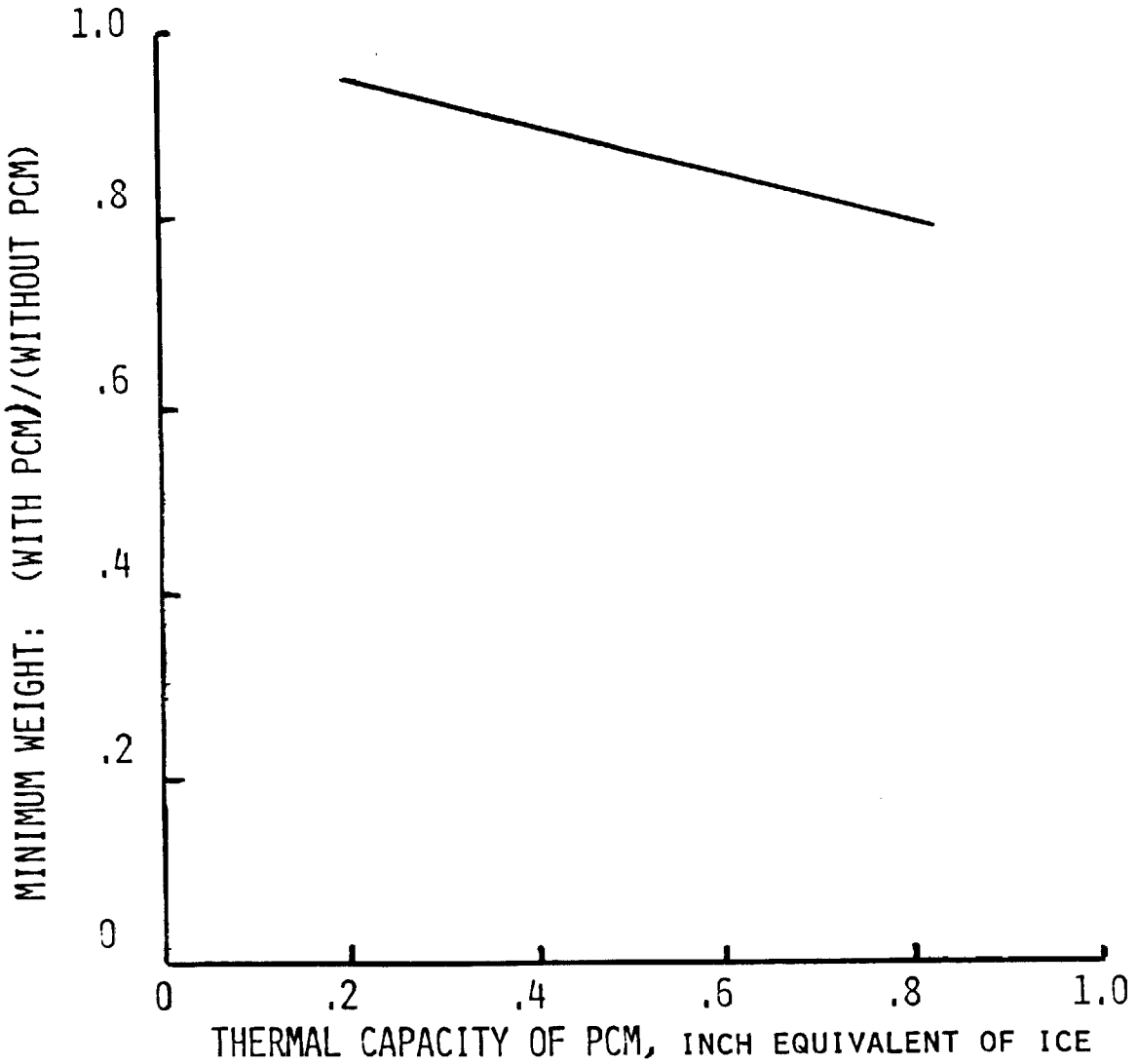

Figure 7. Dependence of minimum weight on thermal capacity of PCM.

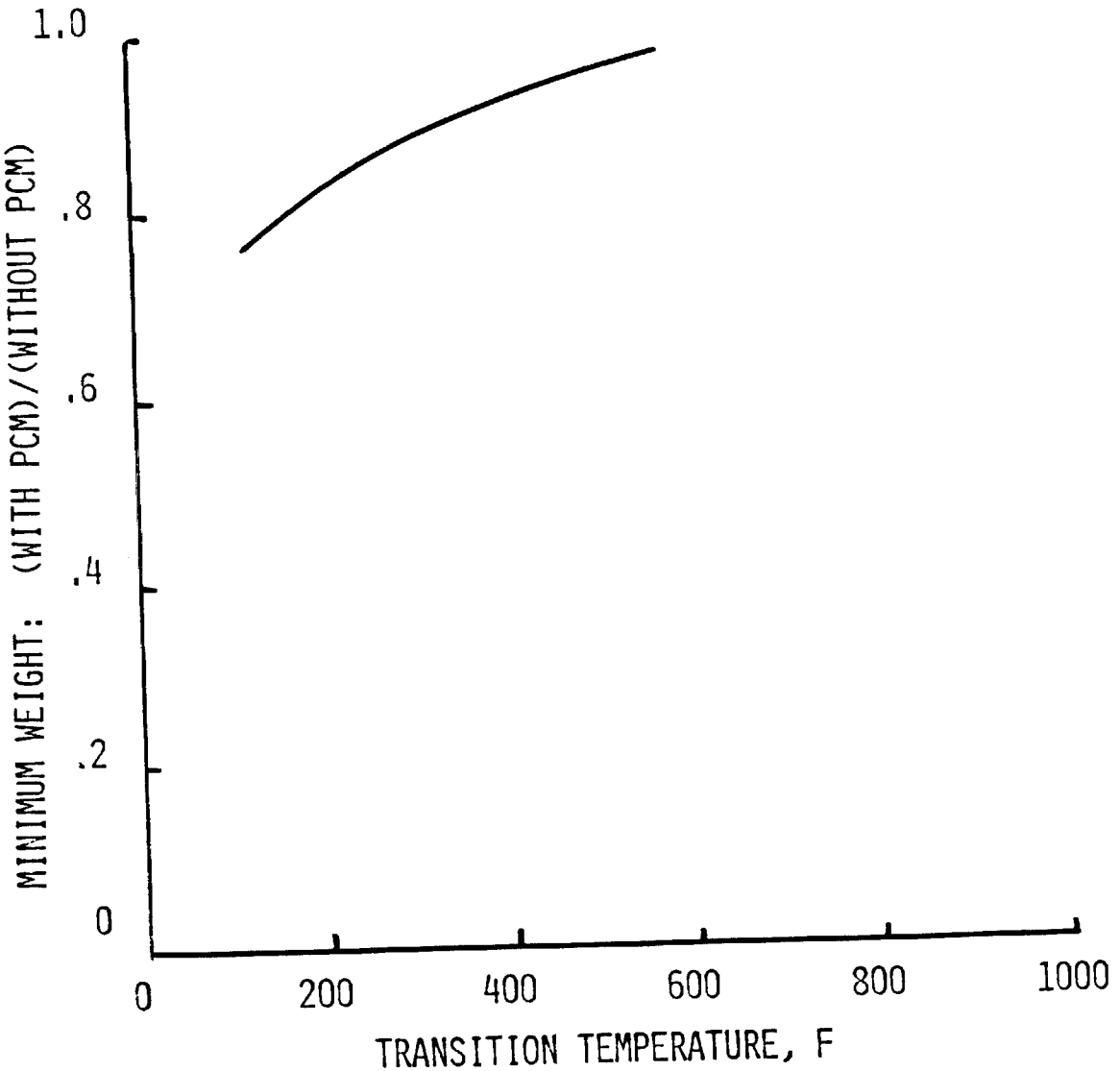

Figure 8. Dependence of minimum weight on transition temperature of PCM.

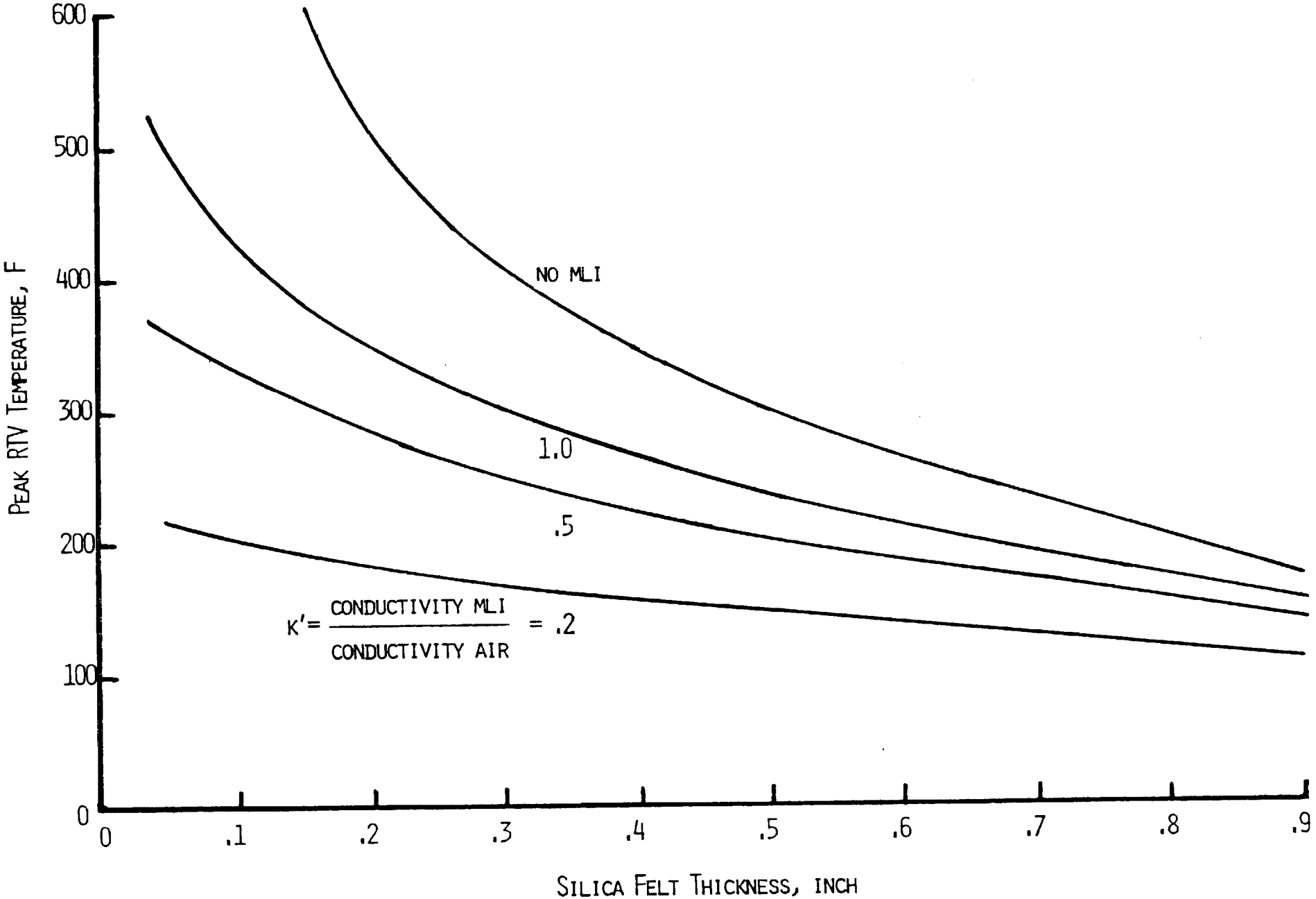

FIG.9 PEAK RTV TEMPERATURE DURING ATMOSPHERE ENTRY.

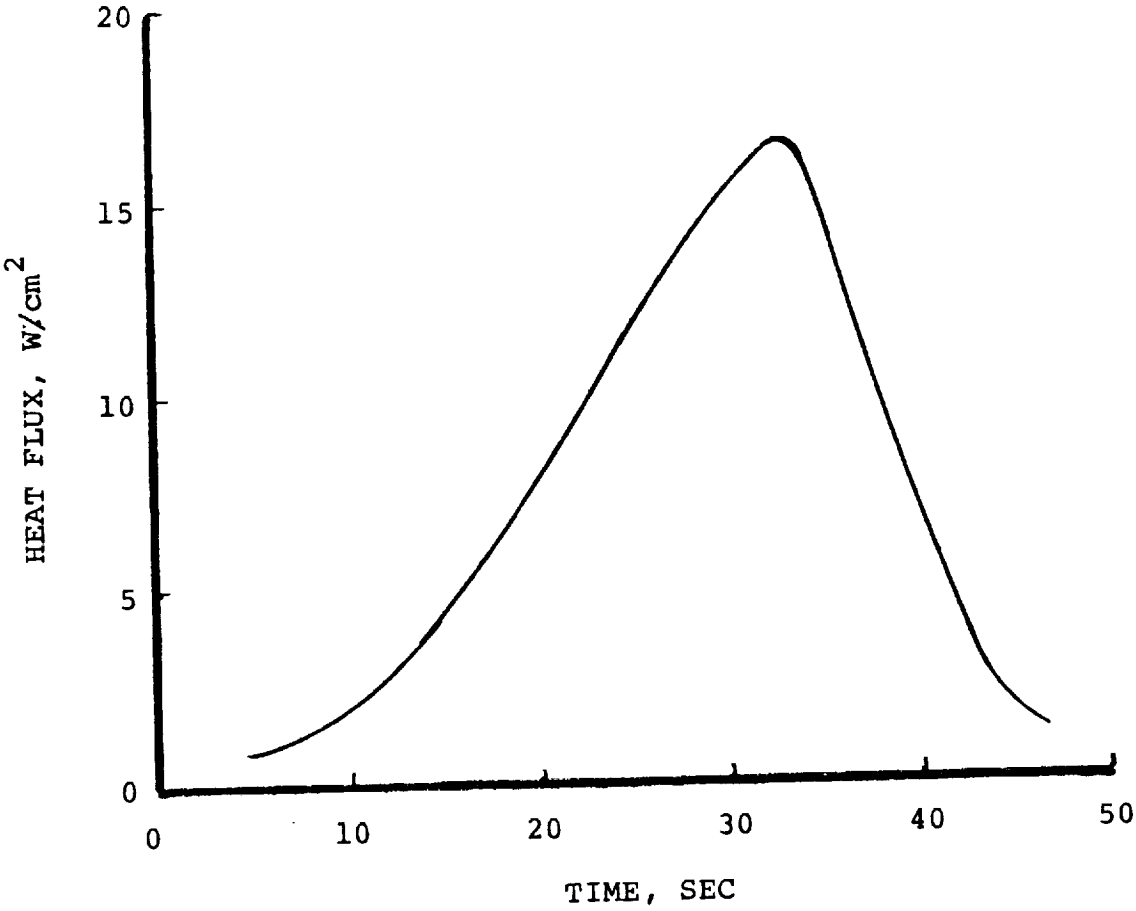

Fig.10- Heat flux imposed to numerical model front surface.

APPENDIX A

MESUR PROBE DESIGN REPORT

Aerothermodynamic Heating Environment

and

Heat Shield Preliminary Design

by

W. D. Henline
NASA Thermal Protection Materials Branch

W. C. Pitts
Eloret Institute

and

Y. K. Chen
Sterling Software

Introduction

This design report presents the results of a study performed at the request of the Ames Research Center Space Projects Division for the Phase A design of the thermal protection system (heatshield) for the proposed Mars MESUR entry probe. At this stage of the project, several mission scenarios are undergoing study. The general mission profile envisions launching separate probe vehicles over a period of time within a given launch window of opportunity. Presently this situation results in two specific design constraints regarding heat shield design. Within the bounds of the above mission profile, there are two (2) probe entry trajectories which effect design. These include a "low" speed direct entry at 7 km/sec and a "high" speed entry at 9 km/sec. The MESUR project office has defined the probe size and shape to be a scaled down version of the 70 degree sphere-cone Mars Viking probe shape. This configuration is shown in Figure 1.

For a Phase A preliminary heat shield design, the following approach was used. Given the entry trajectories, engineering level simulation codes were used to define the aerothermodynamic heating environment for the MESUR probe in the predominantly CO2 atmosphere of Mars. These calculations determined the surface heating distribution over the probe for peak heating conditions. From the heating distributions, stagnation point and off-stagnation point material thermal response calculations were performed over entry trajectory up to the instant of planned heatshield ejection. This procedure was done for the different, most promising thermal protection system (TPS) materials for this application. TPS heat shield thicknesses are obtained for each candidate material, and probe TPS aeroshell options are presented. A more detailed description of each of these procedures is given in the following report.

I. Aerothermodynamic Heating Environment

Trajectories:

M. E. Tauber of the Ames Aerothermodynamics Branch has performed a trajectory analysis for the proposed 7 km/sec and 9 km/sec direct entry MESUR cases. A plot of altitude vs. trajectory time for these profiles is shown in Figure 2 and Figure 3 presents the corresponding stagnation point cold-wall convective heating curves for each entry speed for the MESUR probe shape. Peak heating occurs at 38 sec. into entry for the 7 km/sec case and at 30 sec. for the 9 km/sec entry. For these entry speeds and given the relatively small nose radius of the probe, radiative surface heating is negligible for this mission. Peak heating distributions of the MESUR probe geometry were determined for each of these two peak heating points in the trajectories. It should be pointed out that for such direct entry trajectories, the total (integrated) heat load for the aeroshell will not be a TPS sizing constraint. These entries are of very short duration (of order 20-30 sec) and the heatshield is ejected at about 120 to 130 sec into the entry. Therefore heat soak is at a minimum, and the probe surface heating distribution at peak heating was assumed to apply for the entire trajectory. Surface heating distribution calculations are discussed next.

Forebody Heating Distribution Calculations:

At the peak heating points of the above trajectories, free stream flight conditions were obtained based on the COSPAR North-Summer-Mean atmosphere (approximately 95 % CO2- 5 % N2). These flight conditions were then used as the basis for engineering level, external body aerothermodynamic shock layer heating calculations. Heating to the MESUR probe body is caused by (primarily) convective and surface chemical energy flux to the surface generated from a forebody hypersonic bow shock wave. The flowfield which must be

properly simulated for this problem consistes of a highly dissociated, partially ionized, non-equilibrium plasma flow between the bow shock wave and the body surface. Mass and energy transport as well as dissociation reaction rate chemistry must be accurately calculated to obtain good estimates for the net heat flux to the probe. Reasonably accurate thermo-chemical models for these phenomena are currently available, and are adequate for the approximate sizing calculations required for Phase A studies. Later more detailed final designs will necessitate that the models be updated and validated.

An additional feature of these flowfields is that length Reynolds numbers are quite large. (approx. 10,000 or larger) Primarily this ensures that the shock layer structure consists of a large inviscid region with a thin, viscous boundary layer imbedded near the surface. Normal protocol would call for a detailed and highly resolved reacting, non-equilibrium boundary layer heating calculation. Unfortunately, such a computation requires specification of non-equilibrium boundary layer edge conditions obtained from either a complete Navier-Stokes calculation or from a reacting inviscid simulation of the flow over the MESUR probe in this CO2-N2 system. At present this type of calculation is not available. Complete Navier-Stokes results will be available in the future.

As a compromise for this study, a reacting fully viscous shock computational method was used. The code employed for this analysis is an updated version of a program developed at Langley Research Center by Gupta (Ref. 1). This program termed VSL (viscous shock layer) is a two-dimensional, axisymmetric simulation of the flowfield, including gas phase finite rate dissociation reactions, mass and energy diffusion under the presumption of a strong shock. A complete set of surface boundary conditions, including catalytic surface atom recombination reactions and an energy balance for a radiatively cooled-adiabatic wall are imposed on the solution. No additional boundary conditions are needed as in the boundary layer simulation. For the MESUR Mars atmospheric entry, thermodynamic and transport properties for the CO2-N2 atmosphere system were installed in the code. The fundamental state of knowledge for CO2 gas phase kinetics in these circumstances is now preliminary. Based

on previous and updated experimental estimates (Refs. 2 and 3), a preliminary gas phase reaction set was selected and kinetic rate constants were included in the VSL program.

A major unknown in this computation, and a significant contributor to surface heating (and thus having a large design impact) is the extent of surface catalysis for atomic recombination for any non-ablating case (e.g. this can be the case for the 7 km/sec entry). Using VSL, both fully catalytic and completely non-catalytic surface computations were performed to bracket the extent of this effect.

To obtain design heating profiles for the MESUR forebody geometry, a final engineering approximation had to be made regarding the VSL program. The probe shape (Fig.1) is that of a very blunt, high angle (70 deg. half angle) sphere-cone. Flying at a zero angle of attack (as in this case) the sonic line for the flowfield will be located at the very edge of the cone. Thus the flowfield is completely subsonic in the region of heating. The properties of the flow near the sonic line can then significantly effect the stagnation point heating and the overall heating distribution. The VSL code does not completely take this effect into account and an adjustment must be made. This was done as follows. In Ref. 4 it was shown that the stagnation point heating to a spherical stagnation point calculated using equilibrium, Newtonian theory, could be related directly to the actual stagnation point heating (in a high Reynolds number flow) on a high angle cone (greater than 60 degrees) by determining the stagnation point velocity gradient from a completely inviscid flowfield solution for the actual cone geometry. Such solutions are available from a code (AMIR) available at Ames. The ratio of the AMIR velocity gradient to the analytical value for the Newtonian case (which is used near the stagnation point in the VSL code) can be used to estimate an "effective" nose radius (larger than the actual geometric value) to be used in the VSL code to account for the effect of the extreme bluntness of the MESUR probe.

Using this methodology, surface heating distributions were obtained at the trajectory peak heating points for the 7 km/sec and

9 km/sec entry cases. These results are shown in Figures 4 and 5. In both cases, distributions are presented for both fully catalytic and non-catalystic surfaces. The effect of blunting is included (based on the above methodology) in the VSL results in the form of doubling the nose radius to an effective value of 1-meter. In both cases, the fully catalytic heating values are considerably greater than the non-catalytic results. Because virtually nothing is known about the actual surface catalycity of various TPS materials in the CO2-N2 environment, the conservative fully catalytic heating results are used in this study for design purposes. Future research in this area may provide information in time for a more detailed final design should that be necessary. As can be seen from Figures 4 and 5, the 9 km/sec stagnation heating rates are about twice those for the 7 km/sec values. The heating values and distributions given here (for R_N(effective)=1.0 meter) were used directly in heat shield conduction and sizing calculations for those situations which did not include surface ablation. The distributions themselves were used as scaling functions in surface response and ablation calculations. Based on this information a complete set of conduction, ablation and thermal respose computations were performed for a selected set of appropriate candidate heatshield materials. This is detailed in the following sections.

II. Material Thermal Response Computations.

Non-ablative Conduction Calculations:

For the two different entry cases considered here, only the 7 km/sec case offers the possibility of using a completely radiatively cooled, non-ablating TPS material. Referring to Fig. 4, peak stagnation heat flux is about 75 watts/cm2. Using shuttle tile technology, this translates to a surface temperature of about 3000 F for an adiabatic wall assuming a fully catalytic surface. Although this temperature range is slightly above the current use limits of NASA RSI (reuseable surface insulation) tiles, conduction and sizing calculations were done to provide useful design

information. For any value of surface catalycity less than a fully catalytic case, surface temperatures will be within limits for RSI tiles. Since the MESUR probe must be designed to (as a worst case scenario) withstand significant surface erosion upon planetary entry during a Martian dust storm, design calculations were done here for a toughened version of RSI tile known as AETB-8 (TUFI). This material is a matrix of silica and alumina fibers wherein the surface portion of the tile has been densified with pure silica particles. Ordinary shuttle tiles will not have acceptable erosion rates. Using the aforenmentioned Fig. 4 heating distribution, these heating values were scaled over the trajectory (cold-wall) heating pulse shown in Figure 3. A thermal conduction program developed by the Thermal Protection Branch was used to determine in-depth temperature profiles for specified TUFI tile thicknesses. It was determined that a tile layer of the minimum manufacturable thickness of 0.25 inches would maintain the TPS bond line temperature to less than 350 F. As an example of the in-depth temperature profiles calculated for this material, a plot is shown in Fig. 6 for the body station at 0.5 meters.

In addition to RSI tile technology, previously flown (Viking) elastomeric silicone material known as SLA-561 (manufactured by the Martin Marietta Corp.) is a very light weight (initial density of 14 lb/ft3) low temperature ablative material which can be used in this 7 km/sec trajectory case. This material can operate successfully for heat fluxes up to about 100 watts/cm2. It will not, therefore, be applicable in the stagnation region of the MESUR probe for the 9 km/sec entry. Based on published thermophysical property data for this material (Ref. 5) an ablation-surface recession-in-depth conduction calculation was made for the stagnation point of the MESUR probe for the 7 km/sec entry. These calculations were done using the well known CMA thermal response/ablation code. (Ref. 6) Results from this exercise indicated that SLA-561 operates (in this case) as a pyrolyzing (gas producing), ablator only , and experiences no surface recession. The pyrolysis gas produced provides some measure of surface convective energy blockage. It was also found that (at the stagnation point) 0.375 inches of SLA-561 would maintain the bondline within temperature limits. Additional results

of this computation are presented in Fgures 7 and 8 in the form of stagnation point surface temperature along the entry trajectory and also temperature vs. time and depth, respectively. Figure 9 also shows in-depth temperature profiles for SLA-561 on a dimensionless basis for the body station at 0.67 meters. The minimum material thickness at this location is 0.12 inches. As a check, purely conductive calculations using the Thermal Protection Branch conduction code (no pyrolysis considered) were performed for SLA-561. These results were in agreement with the CMA results, with slight differences due to the lack of pyrolysis modeling.

Conduction calculations were performed for both RSI (AETB-8/TUFI) and SLA-561 on the cone skirt section of the probe beyond a body station of 0.64 meters for the 9 km/sec entry. This was done because heat fluxes in this region are below ablative values for these materials. Note that any increased heating in this region due to turbulence is not a factor for the flowfields encountered here. It was found that the minimum thicknesses determined above would suffice for this portion of the probe in the 9 km/sec case. As demonstrated later, using these materials in this region of the probe can save weight.

Ablative/In-depth Thermal Response:

Referring to Fig.5, fully catalytic heat fluxes are seen to be above 100 watts/cm2 over a significant portion of the MESUR probe for the 9 km/sec entry (peak heating). For this reason CMA ablation thermal response calculations were performed for a higher performance ablative TPS material known as AVCOAT -5026 (TM by the AVCO Corporation). This is a low to moderate density ablator which was used as the manned Apollo capsule heatshield TPS material. There are many other ablator materials which can adequately perform in the region contemplated here; however, almost all of these will result in a significantly heavier heatshield. They were thus not considered further. Again using published thermophysical properties for AVCOAT, (Ref. 5) CMA thermal response-ablation calculations were performed for the 9 km/sec

trajectory (Fig. 2). An initial material thickness of 0.325 inches was found to provide enough protection at the stagnation point to keep the TPS/aeroshell bondline temperature below 350-400 F. For this case, recession values and recession rates along the entry trajectory are given in Figure 10. Only 0.03 inches of recession are predicted. Thus most of the material required is for isulative protection. Figures 11 and 12 also show the stagnation point values for surface temperature and in-depth temperature profiles at the stagnation point for AVCOAT.

III. Options for Forebody Heat Shield Configurations.

For each of the two trajectory cases considered here, there are several different possible TPS material arrangements that will satisfy the heatshielding requirements. This occurs primarily because of the significant difference between the peak stagnation heat flux values and the lesser values on the cone skirt. Each of the design options is described below.

7 km/sec Entry Cases:

1) Complete AETB-8/TUFI Heat Shield.

Shown in Fig. 13 is a sketch of a forebody heat shield comprised soley of TUFI. Since a minimum thickness of 0.25 inches is considered as a manufacturing limit, this is shown as the uniform thickness required over the entire surface. In addition, shown by the dashed line, is an allowance for dust erosion at various stations along the heat shield. These allowances were determined from Reference (7). Given these erosion figures, the total stagnation point material thickness becomes 0.362 inches.

2) Complete SLA-561 Heat Shield.

Based on the SLA-561 calculations described above, the required stagnation point material thickness has been chosen as the

uniform thickness requirement over the entire heat shield. This has been done for a minor conservatism and will aid in heat shield construction. More detailed profiling can be investigated in the final design phase. Figure 14 shows the heat shield configuration, base material thickness and dust erosion allowances for the SLA-561 TPS case.

3) SLA-561 and AETB-8/TUFI Hybrid Heat Shield.

As an option to the two previous designs, Figure 15 shows a possible configuration using SLA-561 in the stagnation region and TUFI tiles on the cone skirt. This option is suggested should it ultimately be desired to use RSI tile technology, with the caveat that these materials may not withstand the higher stagnation region surface temperatures. Material thicknesses and erosion allowances are shown, based on the above described calculations. The material breakpoint occurs at a body station of 0.2 meters.

9 km/sec Entry Cases.

There are three possible design options using the materials selected for this study. These are,

1) Complete AVCOAT-5026 Heat Shield.

This configuration, shown in Figure 16, is presented as the most conservative case for the 9 km/sec entry. Using the stagnation point CMA calculation result for minimum thickness (0.325 inches) as a probable manufacturing minimum, this amount is shown as the requirement over the complete heatshield. Again, additional erosion allowances from Ref. (7) are given, resulting in a total stagnation point AVCOAT thickness of 0.55 inches.

2) AVCOAT/SLA-561 Hybrid Heat Shield.

As an option to save weight and use only materials which have been flown previously, Figure 17 shows a combined heat shield with AVCOAT material in the stagnation region and SLA-561 on the cone skirt. The material change-over point occurs at body station locations beyond 0.64 meters. The previously calculated minimum thicknesses are shown in Fig. 17 together with the associated erosion allowances.

3) AVCOAT/AETB-8(TUFI) Hybrid Heat Shield.

This last option shown in Figure 18 is the same as the previous one except that RSI (AETB-8) TUFI tiles are substituted for the SLA-561 ablator. The tile portion of this design is thinner than SLA but more detailed design and testing will be required to finalize its design. A minimum base thickness of 0.25 inches is shown for the TUFI portion, and required erosion allowances are also shown in Fig. 18.

IV. Heat Shield Weight and Probe Vehicle TPS Mass Fractions

Using the initial material (or absolute) densities for each of the TPS systems discussed above, forebody heat shield total masses were determined based on the MESUR probe geometry. For each of the design cases discussed, TPS mass and associated mass fraction is shown in the following Table.

V_E (km/sec)	m/C_DA (Kg/m^2)	TPS Type	TPS Bulk Density (Kg/m^3)	TPS Mass (Kg)	Structural Mass (Kg)	Total Mass (Kg)	% of 158 Kg Entry Mass
7	30	AETB-8	477.4	15.6	8.97	24.57	15.55
7	30	SLA-561	232.3	11.8	8.97	20.77	13.15
7	30	SLA-561 + AETB-8		14.6	8.97	23.57	14.92
9	30	AVCOAT	544.7	25.4	10.86	36.26	22.95
9	30	AVCOAT + SLA-561		17.5	10.86	28.36	17.95
9	30	AVCOAT + AETB-8		21.2	10.86	32.06	20.29

V. Recommendations for Future Engineering Design Studies.

Should the MESUR program ultimately proceed to the final engineering design stage, then many of the above uncertainties should be eliminated or, at least, reduced in magnitude. There are four (4) major uncertainties at this time. These are 1) surface catalycity for the 7 km/sec entry, 2) the accuracy of the aerothermodynamic simulation of the high angle blunt cone MESUR geometry, 3) particle impact and cratering data for the different candidate TPS materials and 4) the impact of aeroshell flexure on TPS material performance and integrity.

At present, catalytic surface recombination rate coefficients are known only in the air system (O2-N2) and only for the reaction cured glass (RCG) surface of RSI shuttle tiles. No data exists for the CO2-N2 system for any material. Since reduced surface catalycity (cf. Figures 4 and 5) has a potentially dramatic impact on surface heating, there is ample motivation to embark on an experimental program to obtain recombination rate data in Ames arc-jet facilities. This is certainly recommended.

As of now, the Ames Thermal Protection Branch will shortly have finalized a more robust, complete Navier Stokes simulation of the MESUR probe geometry. If this is supplemented with ground based data for validation, it will remove most of the aerothermodynamic simulation uncertainty discussed above.

Most of the dust particle erosion allowances presented here are based on scaling of results known (only approximately) for solid glass fracturing and cratering information. This type of data is essentially unknown for the remaining materials considered. Since these allowances represent a major fraction of the TPS mass, additional data certainly needs to be obtained.

Once more definintive data and TPS designs are obtained in Phase B of the MESUR project, more definitive stuctural dynamics calculations can be performed to aswer questions regarding aeroshell flexure limits on TPS material peformance and structural integrity.

VI. References

1. Gupta, R. N. and Simmonds, A. L., "Stagnation Flowfield Analysis for an Aeroassist Flight Experiment Vehicle," AIAA Paper 88-2613, June, 1988.

2. McKenzie, R. L., "An Estimate of the Chemical Kinetics Behind Normal Shock Waves in Mixtures of Carbon Dioxide and Nitrogen for Conditions Typical of Mars Entry," NASA TN D-3287, 1966.

3. Park, C., Howe, J. T., Jaffe, R. L. and Candler, G. V., "Chemical Kinetics Problems of Future NASA Missions," AIAA Paper 91-0464, Jan., 1991.

4. Stewart, D. A. and Marvin, J. G., "Convective Heat Transfer Rates on Large Angle Conical Bodies at Hypersonic Speeds," NASA TN-5526, 1969.

5. Williams, S. D. and Browning, R. E., Pathfinder Thermophysical Property Data, "Thermal Protection Materials for High Energy Aerobraking Vehicles, Vol. 1, Lockheed Eng. and Sciences Co., Houston TX., NASA Contract NAS 9-17900, Aug., 1989.

6. Aerotherm Charring Material Termal Response and Ablation Program, (CMA87S), Acurex Report UM - 87 - 13/ATD, Nov. 30, 1987.

7. Papadopoulos, P., Tauber, M. and Chang, I., "Heat Shield Erosion in a Dusty Martian Atmosphere," Submitted for presentation at the AIAA Aerospace Sciences Conference, Reno, Nevada, January, 1992.

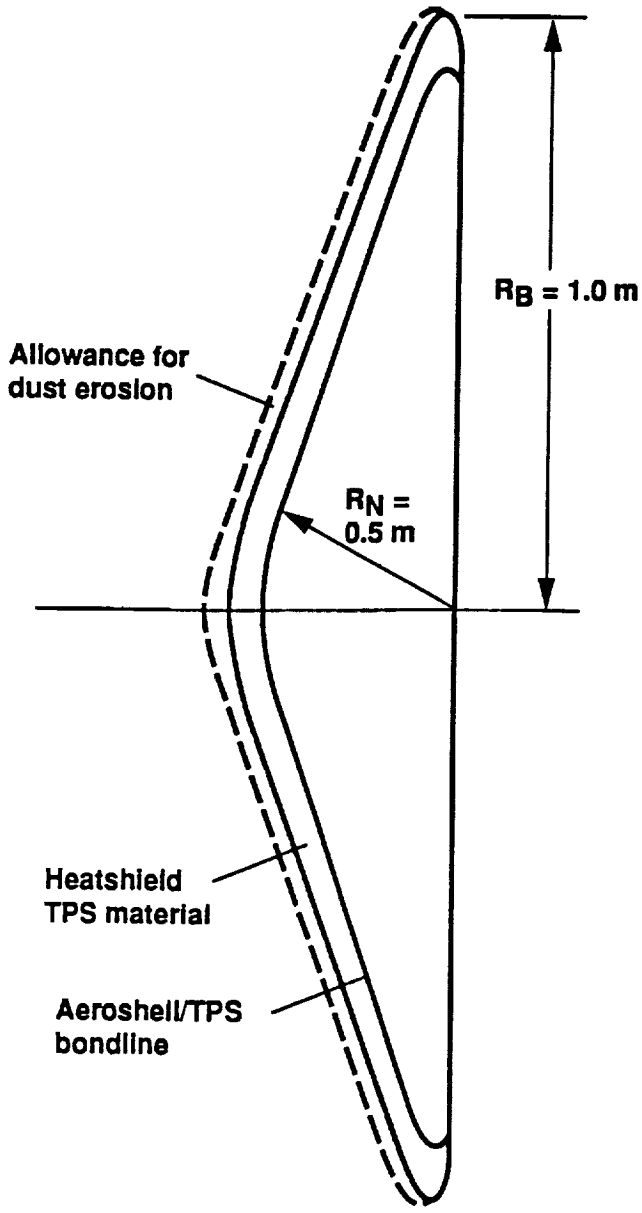

Figure 1. MESUR probe configuration

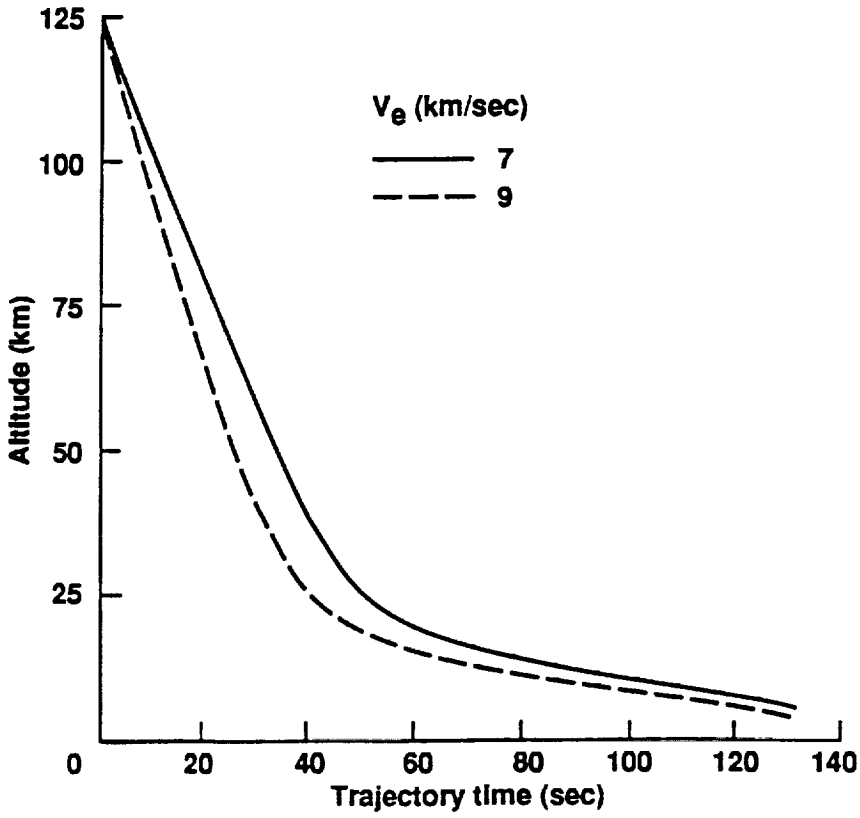

Figure 2. MESUR probe entry trajectories

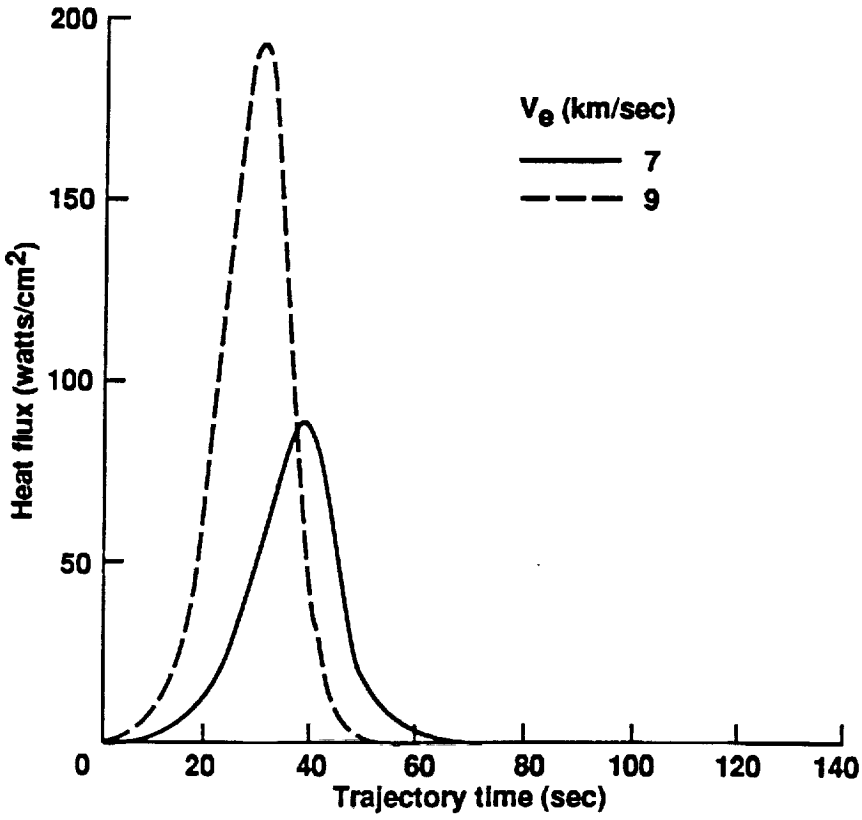

Figure 3. MESUR probe entry cold-wall heating profiles

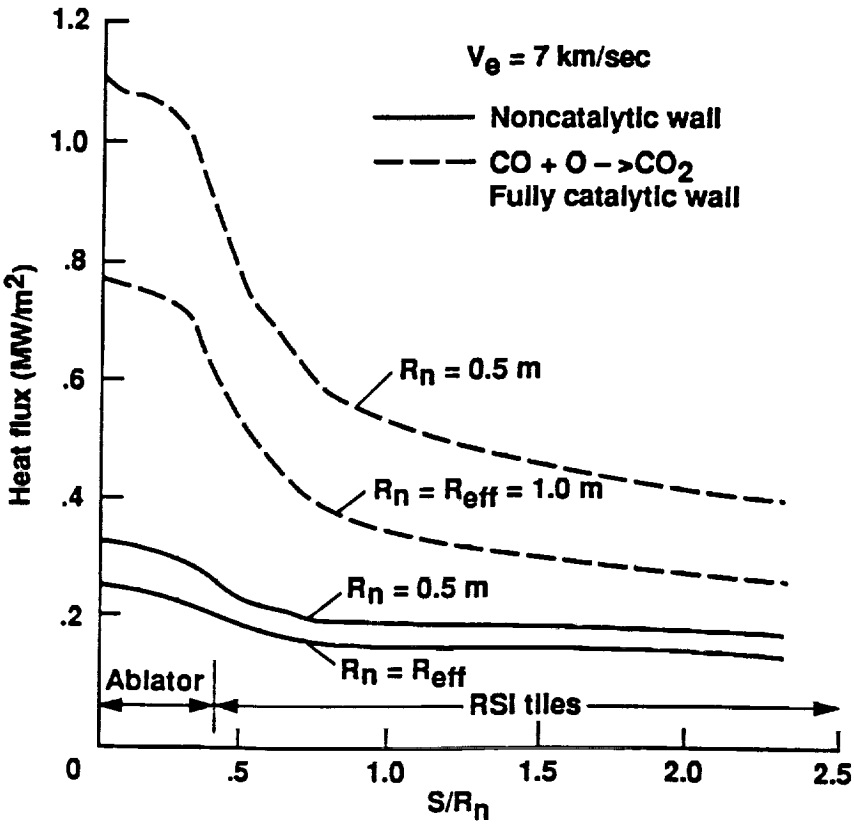

Figure 4: Surface heat flux distributions for 7 km/sec. entry.

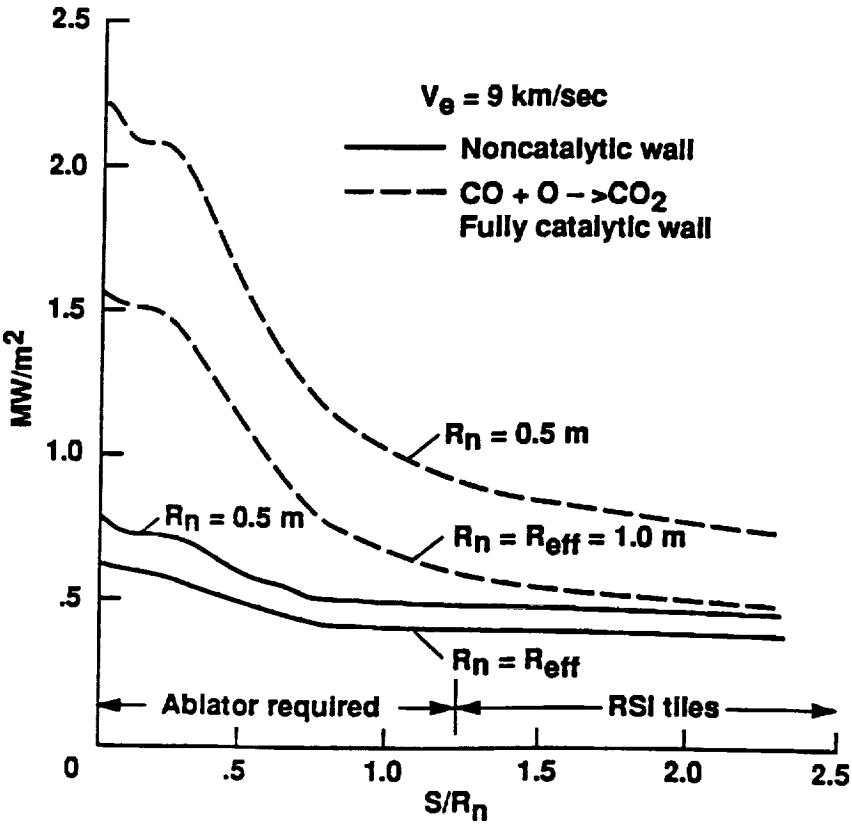

Figure 5: Surface heat flux distributions for 9 km/sec. entry.

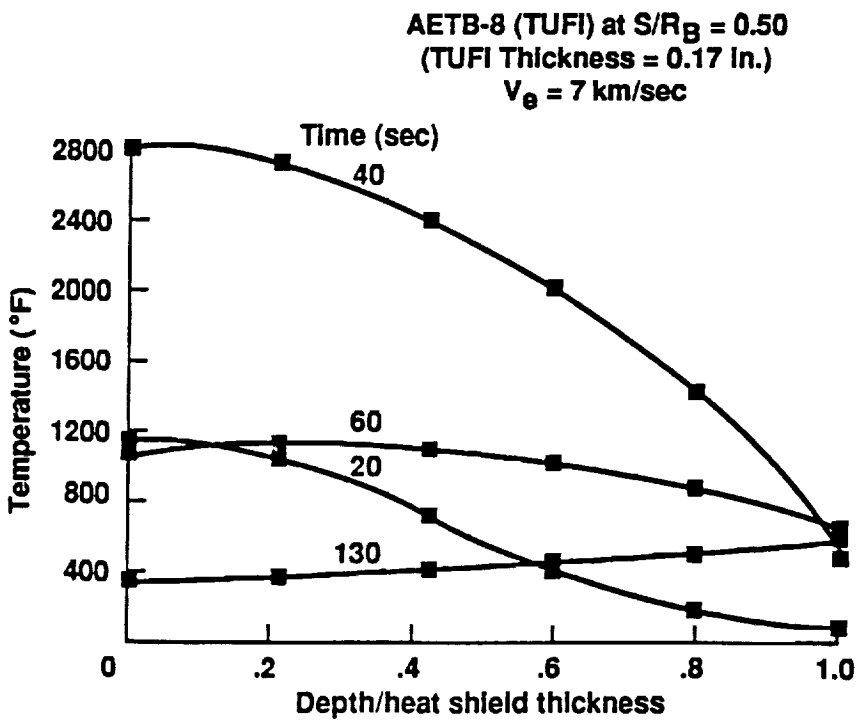

Figure 6. In-depth temperature profiles

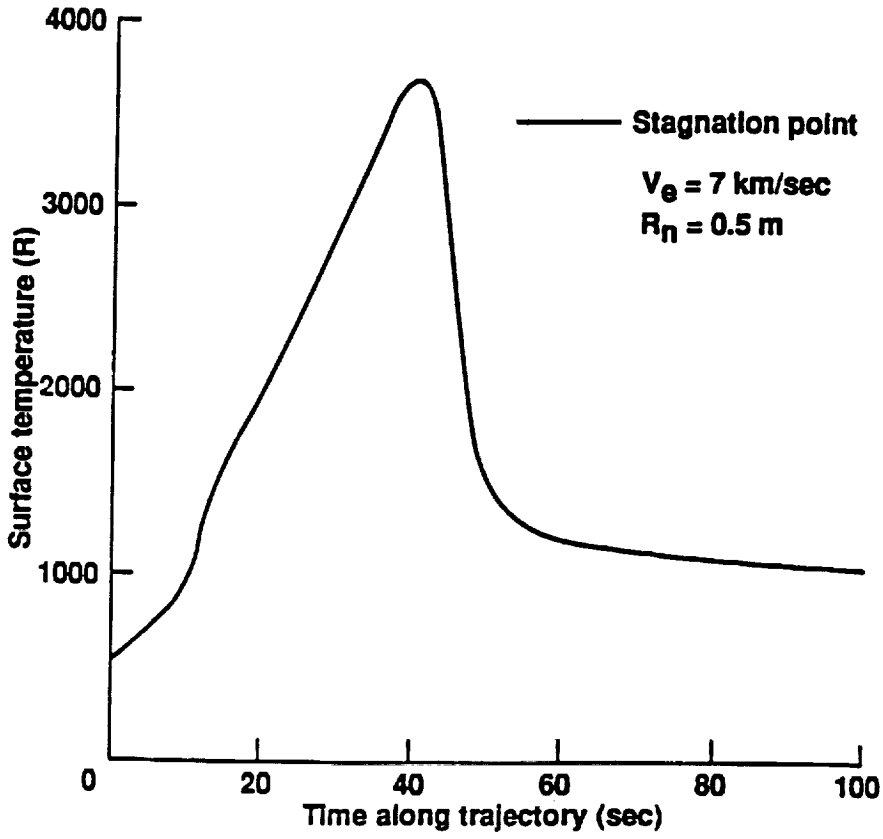

Figure 7. MESUR probe SLA-561 thermal response

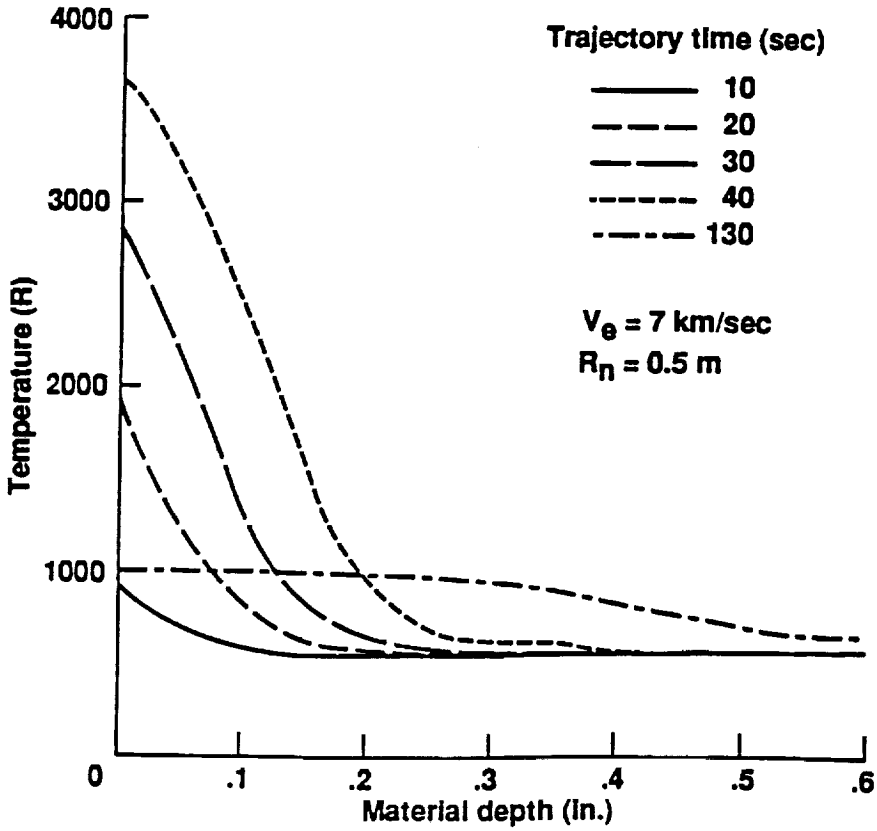

Figure 8: MESUR probe SLA-561 in-depth thermal response.

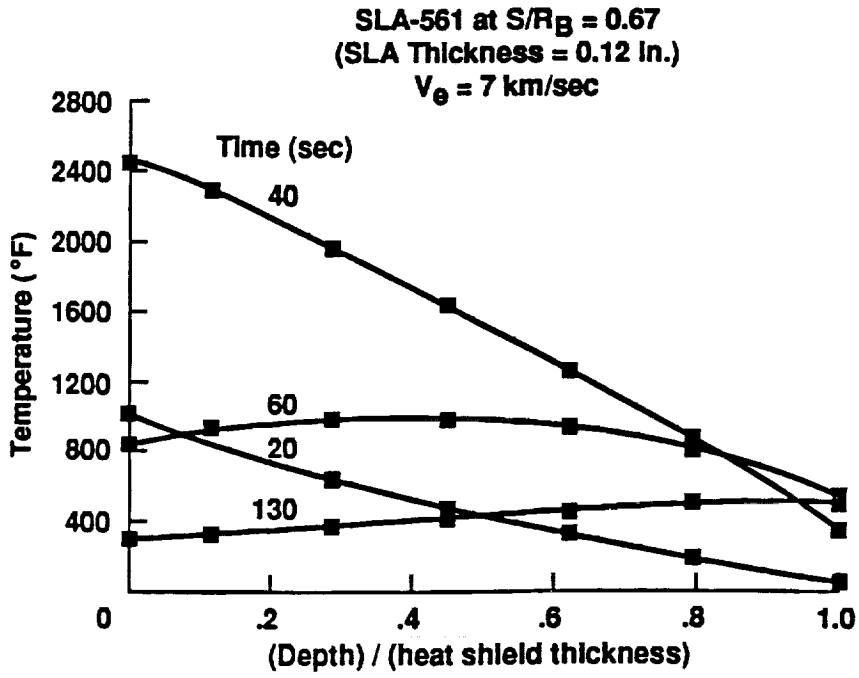

Figure 9: In-depth, off-stagnation temperatures for SLA-561, 7 km/sec.entry.

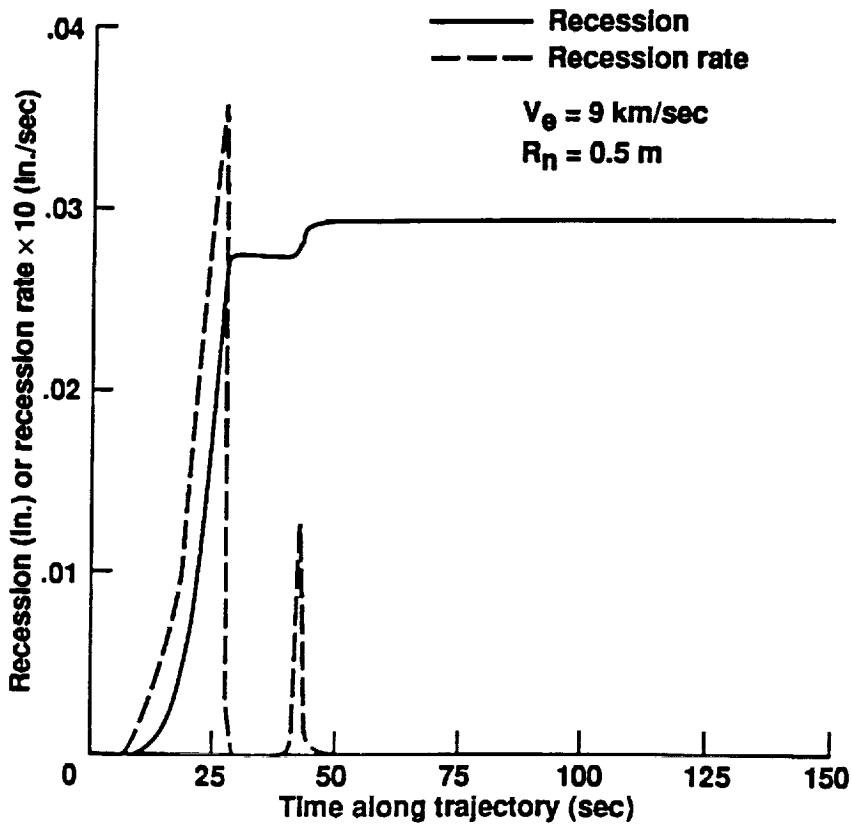

Figure 10: MESUR probe AVCOAT recession.

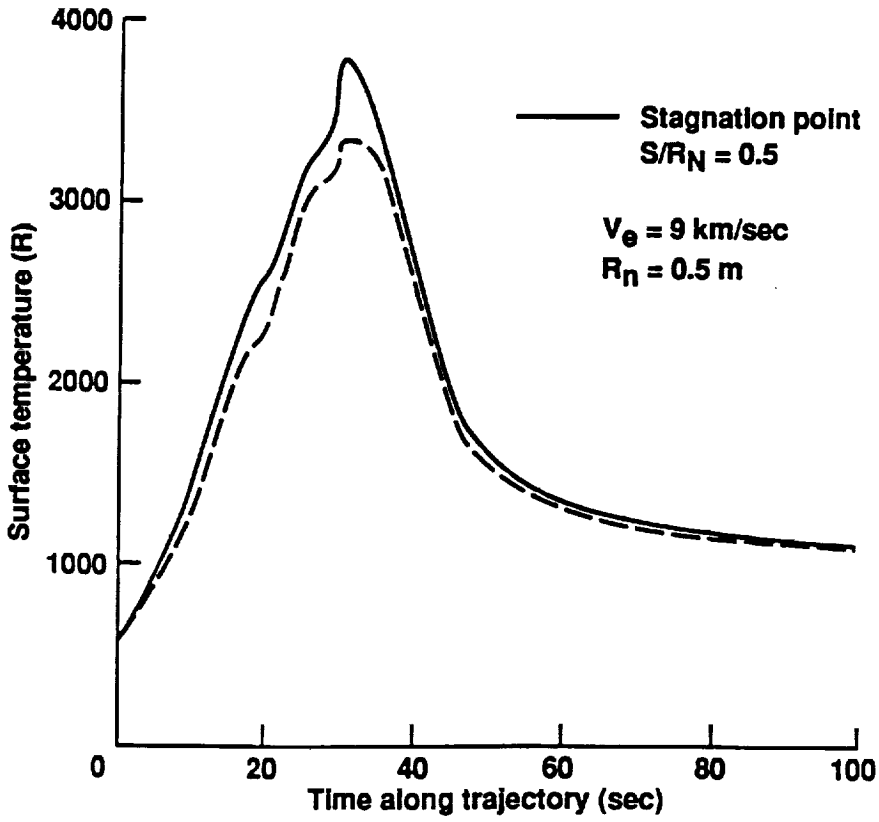

Figure 11: MESUR probe AVCOAT surface thermal response.

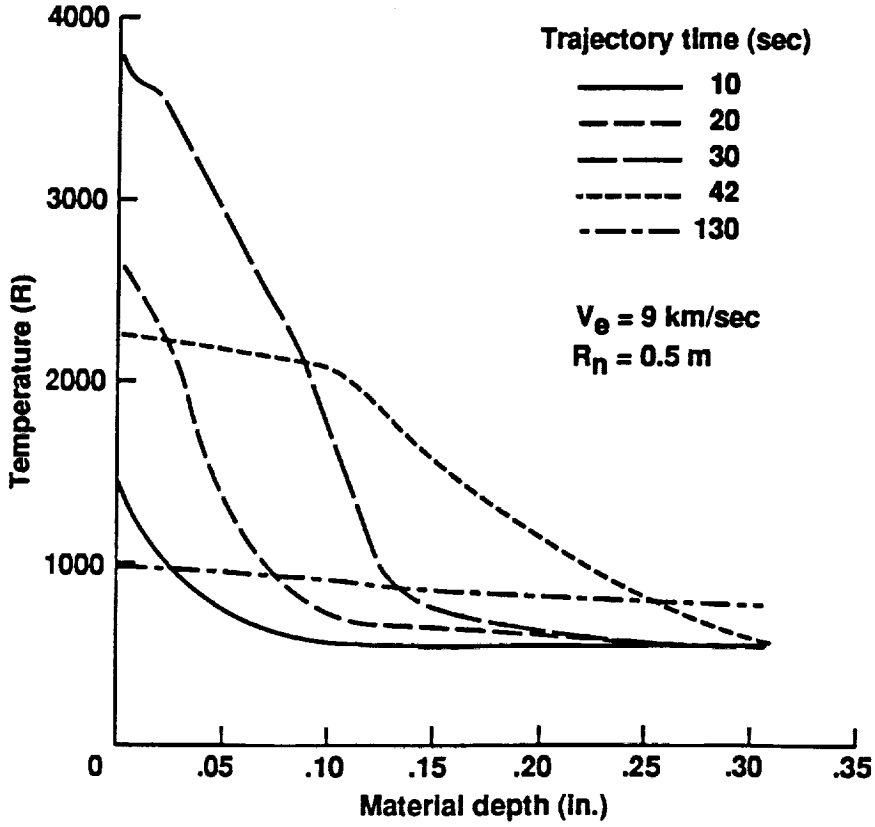

Figure 12: MESUR probe AVCOAT in-depth temperature profiles.

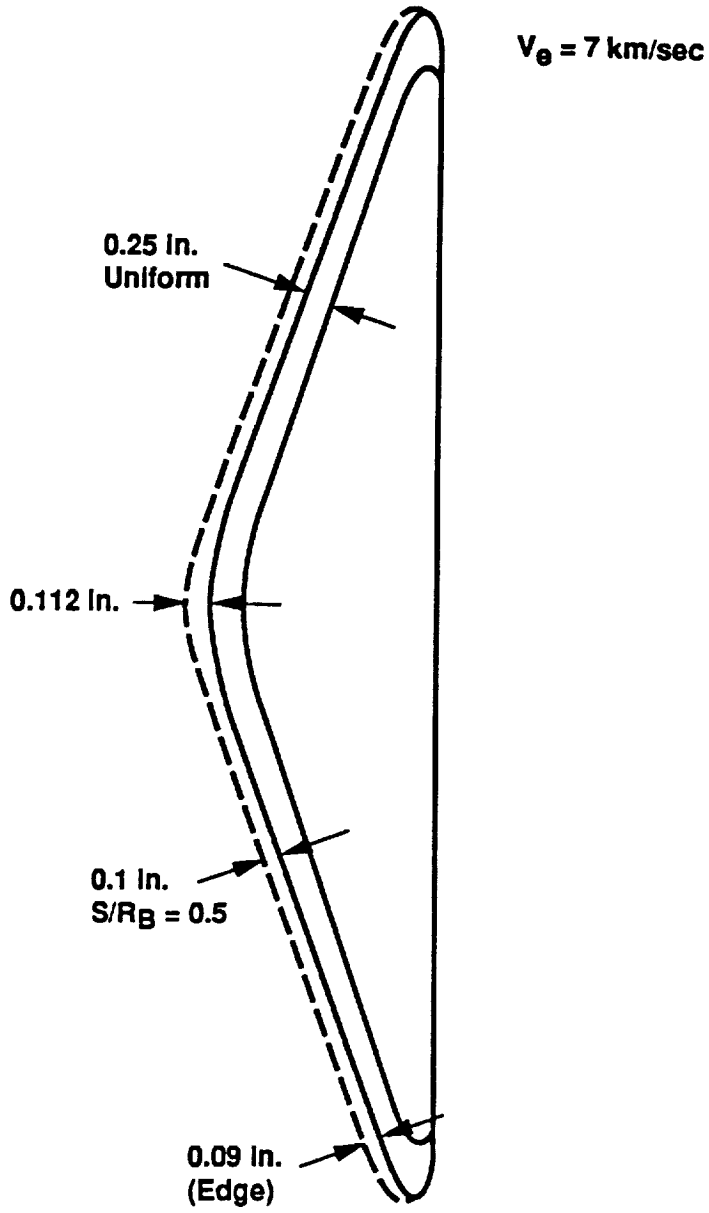

Figure 13. RSI (AETB-8 TUFI) heat shield

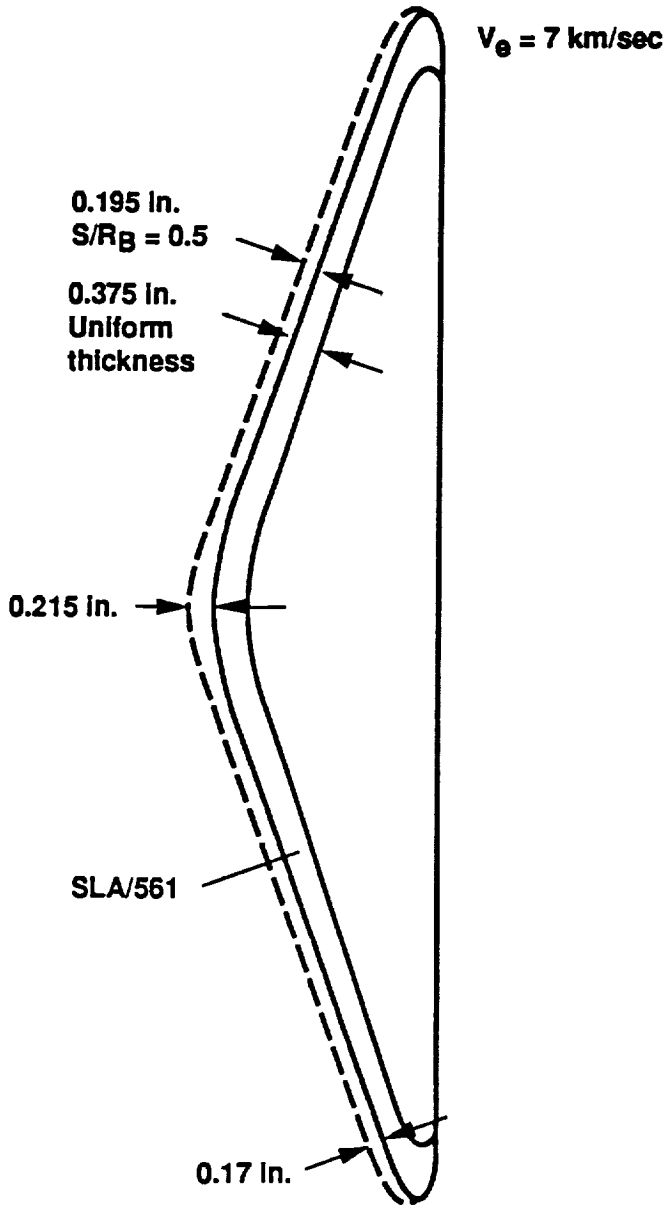

Figure 14. SLA-561 heat shield

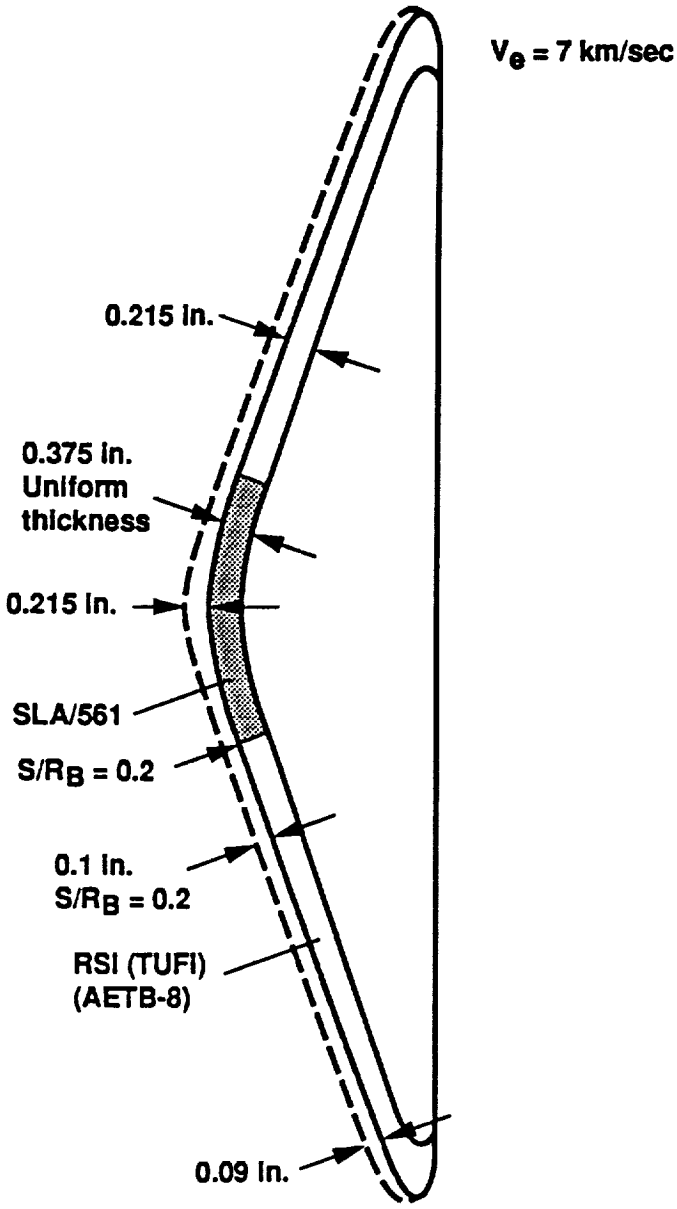

Figure 15: Hybrid SLA-561/RSI heat shield configuration.

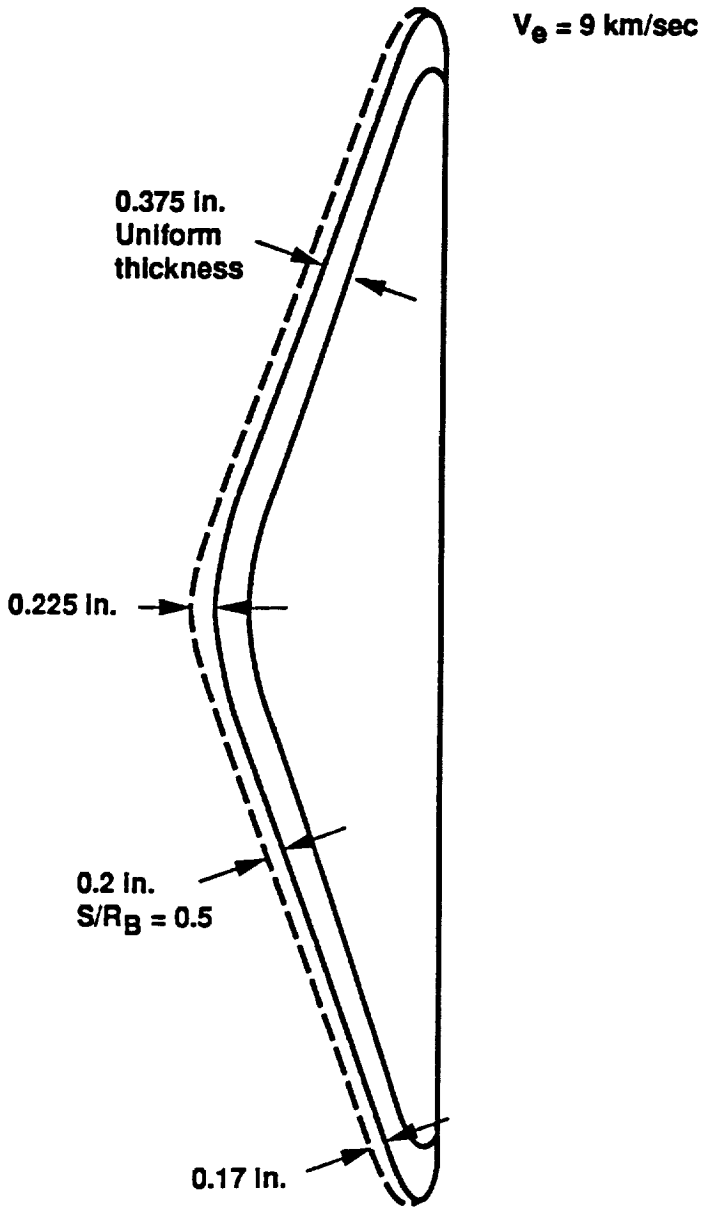

Figure 16: AVCOAT 9 km/sec. entry heat shield configuration.

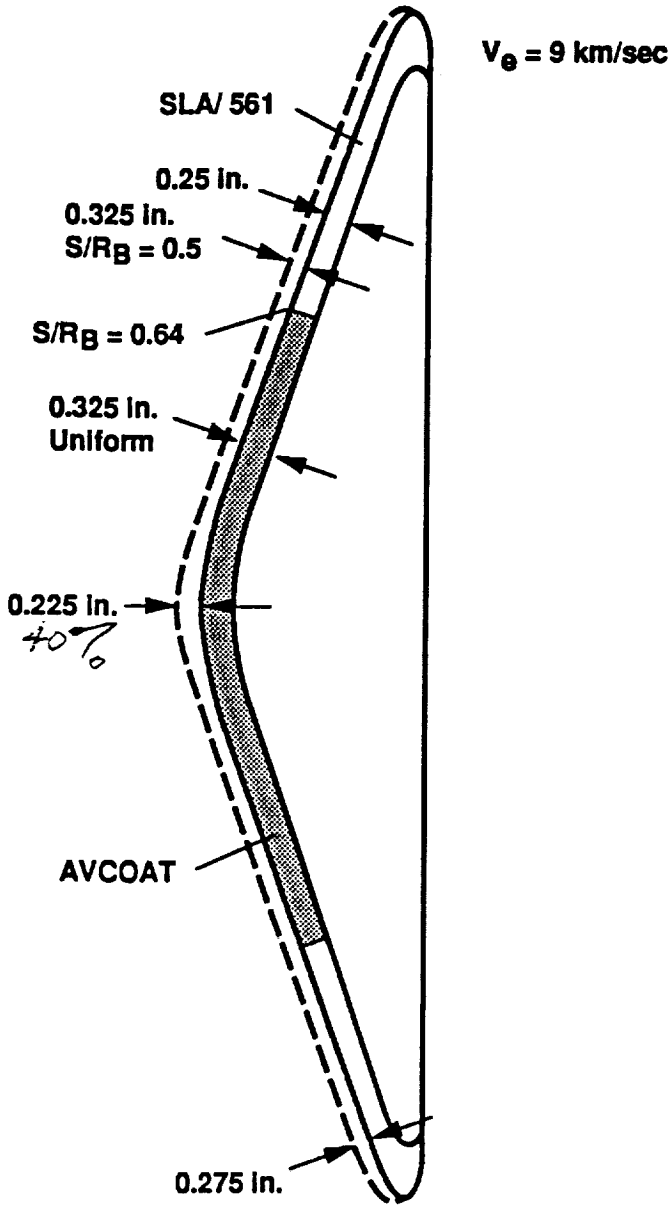

Figure 17: Hybrid AVCOAT/SLA-561 heat shield configuration, 9 km/sec. entry.

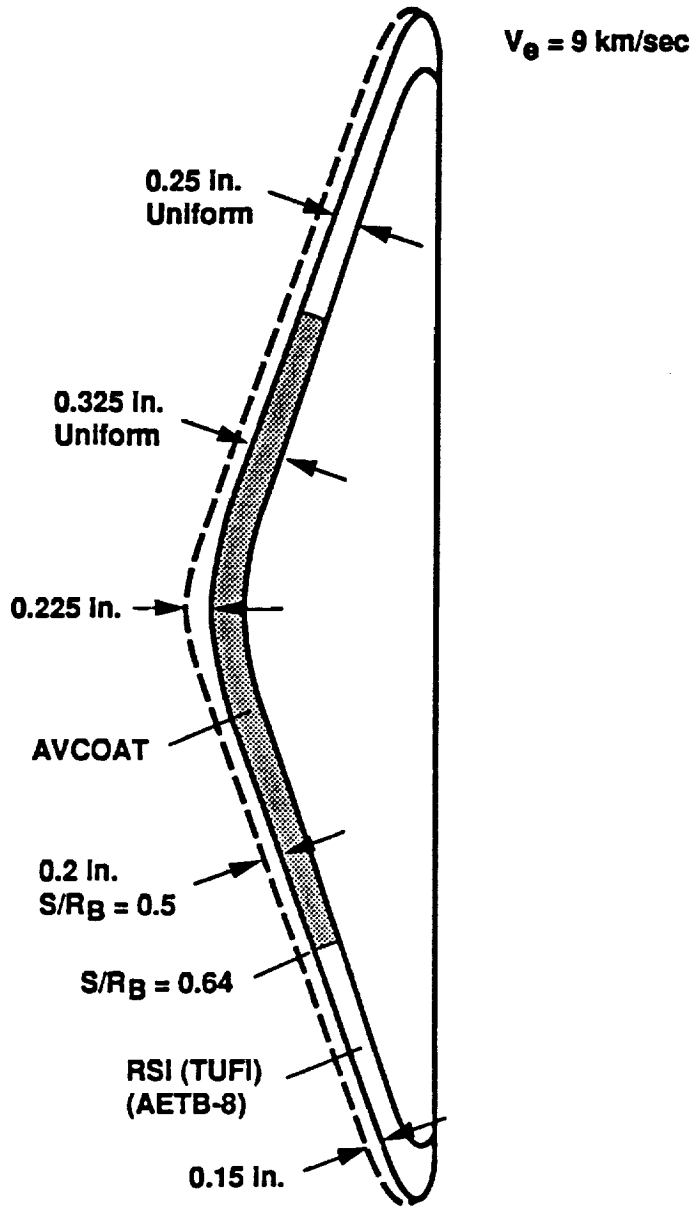

Figure 18: Hybrid AVCOAT/RSI heat shield configuration.